

Enhancing dark siren cosmology through multi-band gravitational wave synergetic observations

Yue-Yan Dong,^{a,1} Ji-Yu Song,^{a,1} Shang-Jie Jin,^{a,b} Jing-Fei Zhang^a
and Xin Zhang^{a,c,d,2}

^aKey Laboratory of Cosmology and Astrophysics (Liaoning Province) and College of Sciences, Northeastern University, Shenyang 110819, China

^bDepartment of Physics, University of Western Australia, Perth WA 6009, Australia

^cKey Laboratory of Data Analytics and Optimization for Smart Industry (Ministry of Education), Northeastern University, Shenyang 110819, China

^dNational Frontiers Science Center for Industrial Intelligence and Systems Optimization, Northeastern University, Shenyang 110819, China

E-mail: dongyueyan@stumail.neu.edu.cn, songjiyu@stumail.neu.edu.cn,
jinshangjie@stumail.neu.edu.cn, jfzhang@mail.neu.edu.cn,
zhangxin@mail.neu.edu.cn

Abstract. Multi-band gravitational-wave (GW) standard siren observations are poised to herald a new era in the study of cosmic evolution. These observations offer higher signal-to-noise ratios and improved localizations compared to those achieved with single-band GW detection, which are crucial for the cosmological applications of dark sirens. In this work, we explore the role multi-band GW synergetic observations will play in measuring cosmological parameters, particularly in comparison with single GW observatory data. We used mock multi-band dark siren data from third-generation GW detectors and the baseline Decihertz Interferometer Gravitational-Wave Observatory to infer cosmological parameters. Our analysis shows that multi-band GW observations significantly improve sky localization accuracy by two to three orders of magnitude over single-band observations, although their impact on luminosity distance error remains limited. This results in a substantial improvement in the constraints on matter density and the Hubble constant, enhancing their constraint precision by 60%–90% and 52%–85%, respectively. We conclude that the significant potential of multi-band GW synergistic observations for detecting GW signals and resolving the Hubble tension is highly promising and warrants anticipation.

¹These authors contributed equally to this paper.

²Corresponding author.

Contents

1	Introduction	1
2	Method	2
2.1	Cosmological model	2
2.2	Simulation of GW sources	3
2.3	Simulation of GW signals	4
2.4	Calculation of SNR	5
2.5	Fisher information matrix	6
2.6	Identifying GW events' potential host galaxies	8
2.7	Cosmological parameter inferences	8
3	Results and discussion	11
3.1	Localizations of SBBHs	11
3.2	Constraints on cosmological parameters	11
4	Conclusion	14

1 Introduction

The Hubble tension has emerged as a significant enigma in cosmology in recent years [1–6]. This confusion stems from a more-than- 5σ discrepancy between the values of the Hubble constant (H_0) inferred from the Planck 2018 CMB observation [7] based on the Λ CDM model (a 0.8% measurement) and obtained through the model-independent distance ladder measurement (a 1.4% measurement) [8]. This inconsistency hints at the possibility of new physics beyond the Λ CDM model (see, e.g., refs. [9–40]). However, no consensus is reached on a valid extended cosmological model that can truly resolve the Hubble tension [18]. Therefore, one may pay more attention to some promising and powerful cosmological probes that can independently measure H_0 to help resolve the Hubble tension. The gravitation wave (GW) standard sirens are a promising new cosmological probe that could help determine the H_0 value independently, which is widely discussed in refs. [41–95] and references therein.

Compact binary coalescence (CBC) events produce GWs whose waveforms encode the luminosity distance information. Through the GW waveform analysis, one can directly obtain the luminosity distance, which is vividly referred to as a standard siren [96, 97]. Once the redshifts of GW sources are determined, the established distance-redshift relation can be used to explore the history of cosmic expansion. There are two main methods regarding the redshift determinations of GW sources adopted by the current GW observations. One is to determine redshift through its electromagnetic (EM) counterparts, an event that relies on the binary neutron star (BNS) or neutron star-black hole (NSBH) merger (usually referred to as a bright siren). The other is to use a galaxy catalog, inferring the redshift through a statistical method (referred to as a dark siren) [92, 98–123].

So far, the first, second, and third observation runs from the LIGO-Virgo-KAGRA (LVK) collaboration have reported over 90 CBC events [124–126]. However, owing to the challenge in detecting EM counterparts, only one bright siren, GW170817, has been identified, which yields approximately a 14% constraint on H_0 [127]. For dark siren analysis, using 46 dark

siren events with SNRs over 11, combined with the GLADE+ catalog [128, 129], achieves a 19% constraint on H_0 [112, 130]. Additionally, the 46 dark sirens combined with the one bright siren GW170817 constrain H_0 to around 10% [112], which has not yet reached the level required to resolve the Hubble tension.

In the future, the multi-band relay detection of a GW event becomes possible. In the few hertz to kilohertz band, the cutting-edge third-generation (3G) ground-based GW detectors, i.e., the Einstein Telescope (ET) [131] and the Cosmic Explorer (CE) [132], are set to debut, anticipated to achieve sensitivity enhancements by an order of magnitude than current GW detectors. The space-based baseline Decihertz Interferometer Gravitational-Wave Observatory (B-DECIGO) [133] with longer arms will provide a detection window in the decihertz band. In addition, GW signals in the millihertz band will be detected by space-based GW detectors with even longer arms, such as LISA [134–136], Taiji [137–139], and TianQin [140–145]. The concept of the multi-band GW observations has been widely investigated in refs. [146–164], and several advantages are dug out: providing early warnings of the detection of BNSs, which is crucial of EM counterparts searches; enhancing the accumulation of signal-to-noise (SNR); improving the precisions of GW parameters inference, including the spatial localization precision.

We notice the current dark sirens analysis with GWTC-3 and GLADE+ catalog has very poor localization, with sky localization primarily a few hundred square degrees, occasionally extending to a few thousand, and high luminosity distance measurement errors, ranging from 40 Mpc to several thousands of Mpc at the 1σ level. We anticipate that in the future, using the multi-band synergetic detection of the GW events will substantially enhance spatial localization precision, thereby improving the precision of constraints on cosmological parameters with dark sirens. Therefore, we wish to study how multi-band synergetic detection of GW events enhances the dark siren cosmology.

In this paper, we simulate the multi-band synergetic detection of B-DECIGO and 3G ground-based GW detectors for the stellar-mass binary black hole (SBBH) GW events. We use the mock galaxy catalog to provide redshift information for GW dark sirens and employ a Bayesian analysis approach to infer cosmological parameters. By changing the apparent magnitude threshold to simulate galaxy catalogs with different completeness, we analyze the influence of the completeness of the galaxy on our results. By comparing the constraint results of cosmological parameters from multi-band and single-band observations, we explore the role that future multi-band observations will play in the GW dark siren cosmology.

This paper is organized as follows. In section 2, we introduce the methods of simulating the multi-band synergetic detection GW data and the dark siren analysis. In section 3, we give the constraint results and make detailed discussions. The conclusion is given in section 4.

2 Method

2.1 Cosmological model

In the expanding universe, the luminosity distance d_L can be expressed theoretically as

$$d_L(z) = c(1+z) \int_0^z \frac{dz'}{H(z')}, \quad (2.1)$$

where c is the speed of light in vacuum, and $H(z)$ is the Hubble parameter, describing the universe's expansion rate at redshift z .

In the standard model of cosmology, the Λ CDM model, the equation of state parameter of dark energy $w = -1$, and $H(z)$ can be expressed as

$$H(z) = H_0 \sqrt{\Omega_m(1+z)^3 + 1 - \Omega_m}. \quad (2.2)$$

In our GW data simulation, we adopt the Λ CDM model as the fiducial model with $H_0 = 67.27 \text{ km s}^{-1} \text{ Mpc}^{-1}$ and $\Omega_m = 0.3166$ from the constraint results of Planck 2018 TT, TE, EE+lowE [7].

2.2 Simulation of GW sources

In this study, we simulate the detection of SBBHs by future GW detectors. The number of SBBHs within the redshift range from z_L to z_U is given by

$$N_{\text{GW}} = \int_{z_L}^{z_U} R_{\text{obs}}(z) dz, \quad (2.3)$$

where $R_{\text{obs}}(z)$ is the SBBH merger rate at z in the observer frame, which can be further converted to the source-frame merger rate $R_m(z)$ via

$$R_{\text{obs}}(z) = \frac{R_m(z)}{1+z} \frac{dV_c(z)}{dz}, \quad (2.4)$$

where $V_c(z) = 4\pi/3 d_c^3(z)$ is the comoving volume. $R_m(z)$ is related to the formation rate of binary systems through the time delay distribution,

$$R_m(z_m) = \int_{z_m}^{\infty} dz_f \frac{dt_f}{dz_f} R_f(z_f) P(t_d), \quad (2.5)$$

where $R_f(z)$ is the formation rate of the binary system, assumed to be proportional to the Madau-Dickinson (MD) star formation rate [165],

$$R_f(z) = A (1+z)^{2.7} \frac{1}{1 + [(1+z)/2.9]^{5.6}}, \quad (2.6)$$

where A is the normalization factor, determined by the BBH merger rate at $z = 0$, and we set $R_m(0) = 23.9 \text{ Gpc}^{-3} \text{ yr}^{-1}$, which is the estimated median rate of O3 observation [166].

$P(t_d)$ is the distribution of the time delay, and we adopt the exponential form as [167]

$$P(t_d) = \frac{1}{\tau} \exp\left(-\frac{t_d}{\tau}\right), \quad (2.7)$$

where $t_d = t_f - t_m$ is the time delay, with t_m being the merger time, which also corresponds to the look-back time at the redshift z_m . The parameter τ is set to 100 Myr.

We obtain the masses of SBBHs based on the POWER LAW + PEAK model [166, 168], which provides a better fit to the observed mass distribution by capturing both the overall power-law trend and the excess around 30–40 M_\odot , expressed as

$$p(m_1) = [(1 - \lambda_{\text{peak}})B(m_1) + \lambda_{\text{peak}}G(m_1)] S(m_1), \quad (2.8)$$

where m_1 ranges from 5 to 44 M_\odot , and $\lambda_{\text{peak}} = 0.038$. $B(m_1) \propto m_1^{-\alpha}$ represents a normalized power-law distribution with the spectral index $\alpha = 3.5$, while $G(m_1)$ is a Gaussian

distribution with the mean value $\mu_m = 34 M_\odot$. $S(m_1)$ is a smoothing function, which is given by

$$S(m_1) = \begin{cases} 0, & \text{if } m_1 < m_{\min}, \\ \frac{1}{f(m_1 - m_{\min}) + 1}, & \text{if } m_{\min} \leq m_1 < m_{\min} + \delta_m, \\ 1, & \text{if } m_{\min} + \delta_m \leq m_1, \end{cases} \quad (2.9)$$

with

$$f(m) = \exp\left(\frac{\delta_m}{m} + \frac{\delta_m}{m - \delta_m}\right), \quad \delta_m = 4.9 M_\odot. \quad (2.10)$$

The probability distribution of the mass ratio q can be expressed as

$$p(q) \propto q^\beta S(m_1 q), \quad (2.11)$$

with $\beta = 1.1$. The secondary mass of the BBH is determined as a function of the mass ratio q . The remaining parameters, including colatitude θ , longitude ϕ , inclination angle ι , polarization angle ψ , coalescence phase φ_c , and coalescence time t_c are randomly sampled within the ranges $\cos \theta \in [-1, 1]$, $\phi \in [0, 2\pi)$, $\cos \iota \in [-1, 1]$, $\psi \in [0, 2\pi)$, $\varphi_c \in [0, 2\pi)$, and $t_c \in [0, 4]$ yr, respectively.

2.3 Simulation of GW signals

For a GW detector network composed of N GW detectors, the Fourier transform of the time-domain waveform is given by [169, 170]

$$\tilde{\mathbf{h}}(f) = e^{-i\Phi} \hat{\mathbf{h}}(f), \quad (2.12)$$

where Φ is a $N \times N$ diagonal matrix, with $\Phi_{kl} = 2\pi f \delta_{kl} (\mathbf{n} \cdot \mathbf{r}_k)$. Here, δ_{kl} is the Kronecker delta, \mathbf{n} is the propagation direction of a GW, and \mathbf{r}_k represents the location of k th GW detector. $\hat{\mathbf{h}}(f)$ is given by

$$\hat{\mathbf{h}}(f) = [\tilde{h}_1(f), \tilde{h}_2(f), \dots, \tilde{h}_N(f)], \quad (2.13)$$

where $\tilde{h}_k(f)$ is the frequency-domain GW waveform on the k th GW detector, given by

$$\tilde{h}_k(f) = h_+(f) F_{+,k}(f) + h_\times(f) F_{\times,k}(f), \quad (2.14)$$

where $h_+(f)$ and $h_\times(f)$ are the waveform of the GW signal. In this work, we use `Pycbc` [171–173] and the phenomenological inspiral-merger-ringdown (IMR) GW model, `IMRPhenomD` [174, 175], to simulate GW signals. $F_{+,k}(f)$ and $F_{\times,k}(f)$ are antenna pattern functions of the k th GW detector, which are related to both the locations of the GW source and the detector. In this work, we analyze ET, two CEs, and B-DECIGO. CE in the USA has 40 km length of arms, denoted as CE (40 km), while the other in Australia with similar design but shortened 20 km length of arms, denoted as CE (20 km). The pattern functions of the L-shaped CE are given by [176]

$$\begin{aligned} F_+(\theta, \phi, \psi) &= \frac{1}{2}(1 + \cos^2 \theta) \cos 2\phi \cos 2\psi - \cos \theta \sin 2\phi \sin 2\psi, \\ F_\times(\theta, \phi, \psi) &= \frac{1}{2}(1 + \cos^2 \theta) \cos 2\phi \sin 2\psi + \cos \theta \sin 2\phi \cos 2\psi. \end{aligned} \quad (2.15)$$

ET is a triangle GW detector with three 10-km arms, which could be equivalent to three interferometers with a 60° angle between each other, and the pattern functions of one of the interferometers are given by [131]

$$\begin{aligned} F_+^{(1)}(\theta, \phi, \psi) &= \frac{\sqrt{3}}{2} \left[\frac{1}{2} (1 + \cos^2 \theta) \cos 2\phi \cos 2\psi - \cos \theta \sin 2\phi \sin 2\psi \right], \\ F_\times^{(1)}(\theta, \phi, \psi) &= \frac{\sqrt{3}}{2} \left[\frac{1}{2} (1 + \cos^2 \theta) \cos 2\phi \sin 2\psi + \cos \theta \sin 2\phi \cos 2\psi \right]. \end{aligned} \quad (2.16)$$

The other two interferometers's pattern functions are $F_{+,\times}^{(2)}(\theta, \phi, \psi) = F_{+,\times}^{(1)}(\theta, \phi + 2\pi/3, \psi)$, and $F_{+,\times}^{(3)}(\theta, \phi, \psi) = F_{+,\times}^{(1)}(\theta, \phi + 4\pi/3, \psi)$, respectively. The antenna pattern functions of one of the interferometers of B-DECIGO are given by [177, 178]

$$\begin{aligned} F_+^{(1)}(\theta, \phi, \psi) &= \frac{1}{2} (1 + \cos^2 \theta) \cos 2\phi \cos 2\psi - \cos \theta \sin 2\phi \sin 2\psi, \\ F_\times^{(1)}(\theta, \phi, \psi) &= \frac{1}{2} (1 + \cos^2 \theta) \cos 2\phi \sin 2\psi + \cos \theta \sin 2\phi \cos 2\psi, \end{aligned} \quad (2.17)$$

and the other interferometer's pattern functions are $F_{+,\times}^{(2)}(\theta, \phi, \psi) = F_{+,\times}^{(1)}(\theta, \phi + \pi/4, \psi)$. In the antenna pattern functions F_+ and F_\times , the angular parameters θ , ϕ , and ψ evolve with the observation time t . Since our calculations employ waveforms in the frequency domain, we account for this variation by expressing the observation time as a function of frequency, given by $t(f) = t_c - 5(8\pi f)^{-\frac{8}{3}} M_c^{-\frac{5}{3}}$ [179, 180]. The explicit form of the angular parameter evolution can be found in ref. [152].

The specific locations of ground-based GW detectors are referenced in refs. [181, 182], while the design of B-DECIGO can be found in ref. [178]. For more details on each GW detector's antenna pattern functions, refer to refs. [177, 183–186]. In addition, we include various network configurations. These configurations encompass the 2CE network, consisting of two CEs; the ET2CE network, comprising ET and 2CE; the B-DECIGO–ET network, which combines B-DECIGO and E the B-DECIGO–2CE network, involving B-DECIGO and 2CE; and finally, the B-DECIGO–ET2CE network, incorporating B-DECIGO and ET2CE.

2.4 Calculation of SNR

When simulating GW detection, we set the detection threshold of SNR to 8 for both individual detectors and detector networks. This threshold is commonly used in the simulation of GW standard sirens, as it balances the need for sufficient detection confidence while maintaining a reasonable event rate [127, 187, 188]. The SNR of the detector network composed of N GW detectors can be expressed as

$$\rho = \sqrt{\sum_{k=1}^N (\tilde{h}_k | \tilde{h}_k)}, \quad (2.18)$$

where \tilde{h}_k is the GW waveform of the k th GW detector. The inner product is defined as

$$(\tilde{h} | \tilde{h}) = 4 \int_{f_{\text{in}}}^{f_{\text{out}}} \frac{\tilde{h}(f) \tilde{h}^*(f)}{S_n(f)} df, \quad (2.19)$$

where $\tilde{h}^*(f)$ is the complex conjugate of $\tilde{h}(f)$ and $S_n(f)$ is the one-side noise power spectral density (PSD) of the GW detector. Here we adopt the PSD of ET from ref. [189], of CE

(40 km) from ref. [190], of CE (20 km) from ref. [189], and of B-DECIGO from ref. [149]. Moreover, f_{in} and f_{out} are the frequencies at which the GW signal enters and leaves the frequency band of the GW detector, respectively.

In figure 1, we show the characteristic sensitivities of ET, CE (40 km), CE (20 km), B-DECIGO, LIGO in Livingston, and VIRGO (see ref. [130]). Note that the GW190725-like event is shown as the representative since it has the highest calculated SNR of the multi-band observation among the GW events. It can be found that the frequency band of B-DECIGO is well connected with ground-based detectors, enabling the accumulation of a higher SNR across the longer frequency band.

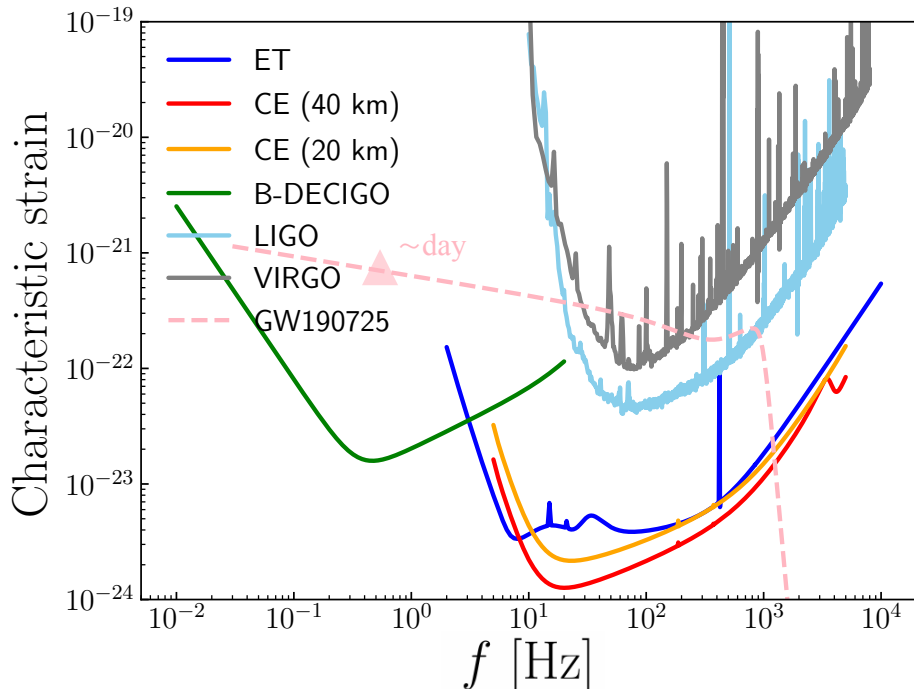


Figure 1. Characteristic strains of ET, CE (40 km), CE (20 km), B-DECIGO, LIGO in Livingston, and VIRGO, together with the effective strain amplitude of GW190725. The pink triangle positions the frequency of the GW signal a day before coalescence. We define the dimensionless characteristic strain as $\sqrt{fS_n}$ for the GW detectors and $2f|h(f)|$ for the GW source.

In figure 2, we show the corresponding detection horizons for equal-mass non-spinning binaries from ET, CE (40 km), CE (20 km), and B-DECIGO, based on the total mass in the source frame, with $\text{SNR} > 8$. We can find that, for B-DECIGO and 3G ground-based detectors, multi-band synergetic detection is achievable for both SMBHs and light intermediate-mass black holes.

2.5 Fisher information matrix

We use the Fisher information matrix (FIM) [191] to simulate the GW source parameters' measurement errors. For a GW detector network with N interferometers, the FIM is given

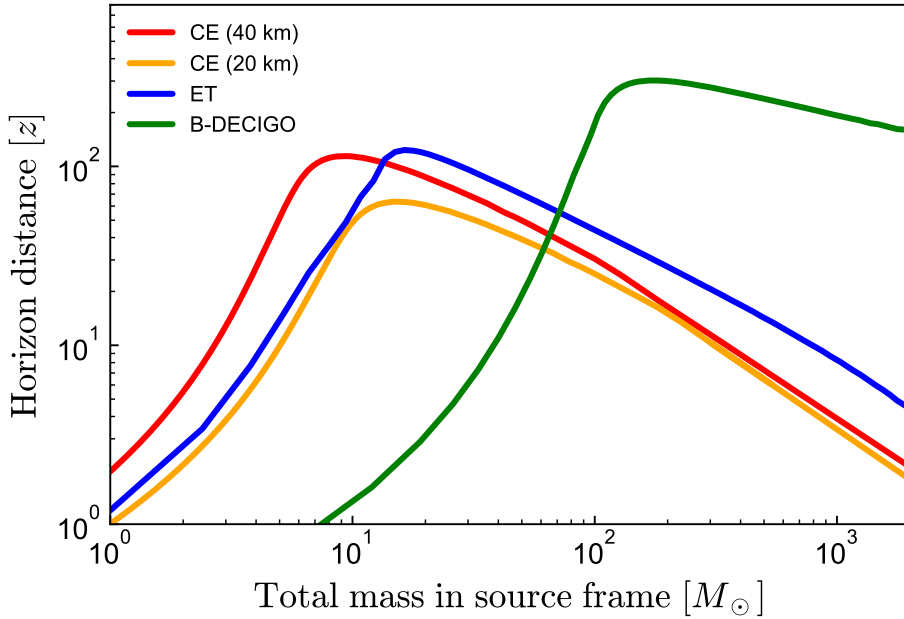


Figure 2. Detection horizons for the equal-mass non-spinning binaries as a function of the source frame total mass for ET, CE (40 km), CE (20 km) and B-DECIGO.

by

$$F_{ij} = \sum_{k=1}^N \left(\frac{\partial \tilde{h}_k}{\partial \theta_i} \middle| \frac{\partial \tilde{h}_k}{\partial \theta_j} \right), \quad (2.20)$$

where θ_i denotes the i th parameter among the nine GW source parameters describing the GW signal, which are $d_L, t_c, \mathcal{M}_c, \eta, \theta, \phi, \psi, \iota, \psi_c$. Among them, θ and ϕ represent the colatitude and the longitude of the GW event, respectively. ψ is the polarization angle, ψ_c is the coalescence phase and t_c is the coalescence time.

The 9×9 covariance matrix (Cov) of the GW source parameters is equal to the inverse of the FIM, and the measurement error of the i th GW parameter is given by $\Delta \theta_i = \sqrt{Cov_{ii}}$. The sky localization error is given as

$$\Delta \Omega = 2\pi |\sin \theta| \sqrt{(\Delta \theta)^2 (\Delta \phi)^2 - (\Delta \theta \Delta \phi)^2}. \quad (2.21)$$

The total error of d_L is expressed as

$$\Delta d_L = \sqrt{(\Delta d_L^{\text{inst}})^2 + (\Delta d_L^{\text{lens}})^2 + (\Delta d_L^{\text{pv}})^2}, \quad (2.22)$$

where Δd_L^{inst} represents the instrumental error of d_L , estimated using FIM; Δd_L^{lens} denotes the weak-lensing error, given by [192, 193]

$$\Delta d_L^{\text{lens}}(z) = d_L \times 0.066 \left[\frac{1 - (1+z)^{-0.25}}{0.25} \right]^{1.8}. \quad (2.23)$$

$\Delta d_L^{\text{pv}}(z)$ is the peculiar-velocity error, given by [194]

$$\Delta d_L^{\text{pv}}(z) = d_L \times \left[1 + \frac{c(1+z)^2}{H(z)d_L(z)} \right] \frac{\sqrt{\langle v^2 \rangle}}{c}, \quad (2.24)$$

where $\sqrt{\langle v^2 \rangle}$ is the peculiar velocity of the GW source, set to $\sqrt{\langle v^2 \rangle} = 500 \text{ km s}^{-1}$ [59].

2.6 Identifying GW events' potential host galaxies

We rely on the three-dimensional (3D) localization capability of the GW detector to identify the potential host galaxies of GW sources. In our analysis, we model the 3D localization region of each GW event as a truncated cone, characterized by a radial range of $[d_L^{\min}, d_L^{\max}] = [\bar{d}_L - 3\Delta d_L, \bar{d}_L + 3\Delta d_L]$ and an angular region defined by $\chi^2 \leq 9.21$. Here, \bar{d}_L represents the luminosity distance of the GW event, Δd_L denotes the 1σ error of the luminosity distance measurement, obtained by eq. (2.22), and χ^2 is expressed as

$$\chi^2 = (\theta - \bar{\theta}, \phi - \bar{\phi}) Cov'^{-1} \begin{pmatrix} \theta - \bar{\theta} \\ \phi - \bar{\phi} \end{pmatrix}, \quad (2.25)$$

where Cov'^{-1} is the 2×2 covariance matrix of θ and ϕ . We obtain Cov'^{-1} by removing the rows and columns associated with the other parameters from the original 9×9 covariance matrix estimated through the FIM analysis. The χ^2 value quantifies the deviation of a data point at (θ, ϕ) from the expected position at $(\bar{\theta}, \bar{\phi})$ in terms of angle. The condition $\chi^2 \leq 9.21$ corresponds to the 99% confidence region.

To match with the galaxy catalog, we convert the range of luminosity distances into a corresponding range of redshifts, denoted as $[z_{\min}, z_{\max}]$. Specifically, $z^{\min} = z(d_L^{\min}, H_0^{\min}, \Omega_m^{\min})$ and $z^{\max} = z(d_L^{\max}, H_0^{\max}, \Omega_m^{\max})$, where H_0^{\min} , H_0^{\max} , Ω_m^{\min} , and Ω_m^{\max} are the edge values of prior ranges of H_0 and Ω_m . Here, we set $H_0 \in [20, 140] \text{ km s}^{-1} \text{ Mpc}^{-1}$ and $\Omega_m \in [0.1, 0.5]$. In summary, the potential host galaxies of each GW event are constrained within the range of $[z_{\min}, z_{\max}]$ and $\chi^2 \leq 9.21$. Additionally, following ref. [119], we calculate an angular localization weight for each potential host galaxy using the equation

$$w \propto \frac{1}{2\pi|Cov'|} \exp \left[-\frac{1}{2} (\theta - \bar{\theta}, \phi - \bar{\phi}) Cov'^{-1} \begin{pmatrix} \theta - \bar{\theta} \\ \phi - \bar{\phi} \end{pmatrix} \right]. \quad (2.26)$$

For an intuitive description of the process of identifying potential host galaxies of GW sources, refer to figure 3. It is worth noting that the angle weighting approach is only applicable in simulated data research. This is because the source parameter posterior in simulated data is assumed to be Gaussian, and the error is calculated through FIM. In real data research, however, the source parameter posterior is non-Gaussian, so angle weighting isn't feasible.

2.7 Cosmological parameter inferences

Inferring cosmological parameters using GW dark sirens requires redshift information from galaxy catalogs. In this work, we generate a simplistic galaxy catalog by uniformly sampling galaxies within the comoving volume with a number density of 0.02 Mpc^{-3} (the median value of the result of ref. [195]). We explore the impact of the galaxy catalog's completeness on cosmological parameter inference by changing the apparent magnitude threshold to mock galaxy catalogs with different levels of completeness. For redshift uncertainties of galaxies in the mock galaxy catalog, we ignore the redshift measurement errors for galaxies at $z \leq 0.1$ assuming these galaxies could be covered by future spectroscopic surveys [111, 196], and beyond this range, we mock the redshift uncertainties of galaxies as $\Delta z(z) = 0.02(1+z)$, which is the redshift measurement accuracy could be achieved by future photometric surveys [197].

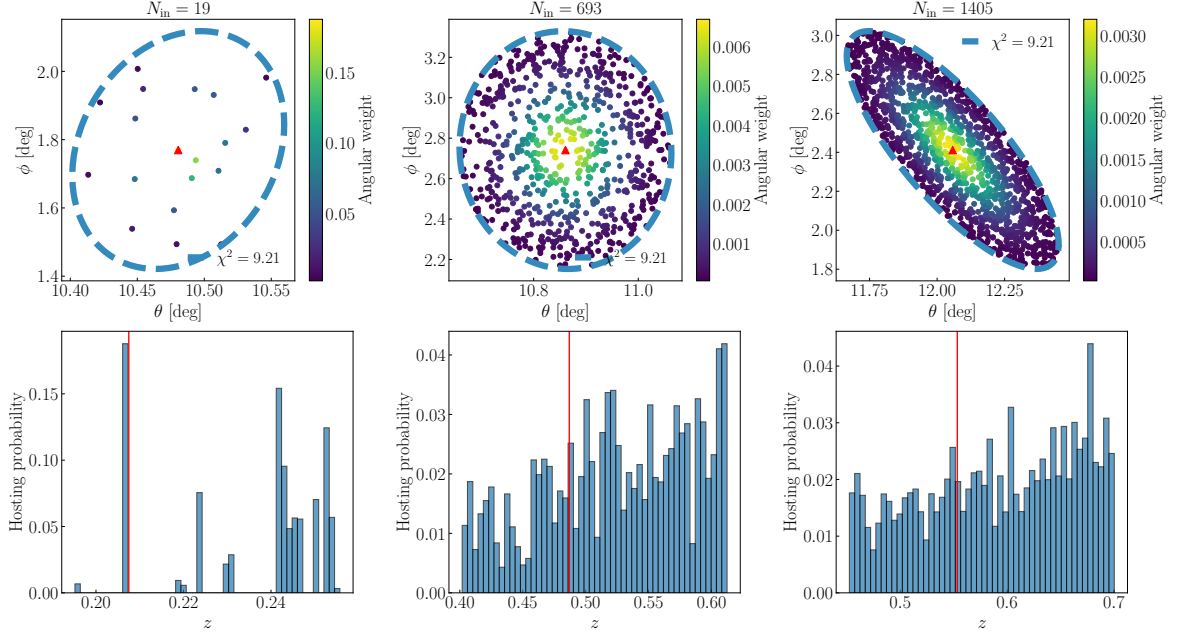


Figure 3. Process of identifying potential host galaxies, with each column showcasing a representative case. The upper panels depict the distribution of potential host galaxies in the θ - ϕ plane. Each point is color-coded according to the angular weight of the potential host galaxy calculated using eq. (2.26). Red triangles denote the sky positions of the true host galaxies. The blue dashed circle represents the range of $\chi \leq 9.21$, calculated through eq. (2.25), corresponding to 99% confidence region. The lower panels show the redshift distributions of potential host galaxies, with the y-axis indicating the probability of hosting GW sources in each redshift bin after using the angular weight. The red lines indicate the redshift of the true host galaxies.

We employ the Bayesian analysis to infer cosmological parameters Ω . The posterior distribution of Ω is given by

$$p(\Omega|\{D_{\text{GW}}\}) \propto p(\{D_{\text{GW}}\}|\Omega)p(\Omega), \quad (2.27)$$

where $\{D_{\text{GW}}\}$ represents the GW dataset $p(\Omega)$ is the prior distribution of Ω . We adopt uniform priors for all cosmological parameters, with $H_0 \in [20, 140]$ km s⁻¹ Mpc⁻¹ and $\Omega_m \in [0.1, 0.5]$. $p(\{D_{\text{GW}}\}|\Omega)$ is the likelihood function. As the detection of each GW event is independent, the likelihood function of the GW data set $\{D_{\text{GW}}\}$ can be expressed as the product of individual GW event's likelihood:

$$p(\{D_{\text{GW}}\}|\Omega) = \prod_{i=1}^{N_{\text{GW}}} p(D_{\text{GW},i}|\Omega), \quad (2.28)$$

where N_{GW} is the number of GW events. The likelihood function of a single GW event is given by

$$p(D_{\text{GW}}|\Omega) = \frac{1}{\beta(\Omega)} \int \int p(D_{\text{GW}}|d_L)\delta(d_L - d_L(z, \Omega))p(z|\Omega)dzdd_L, \quad (2.29)$$

where $p(D_{\text{GW}}|d_{\text{L}})$ is the posterior distribution of the GW event's d_{L} , given by

$$p(D_{\text{GW}}|d_{\text{L}}) = \frac{1}{\sqrt{2\pi}\Delta d_{\text{L}}} \exp\left[-\frac{(\hat{d}_{\text{L}} - d_{\text{L}})^2}{2\Delta d_{\text{L}}^2}\right], \quad (2.30)$$

where Δd_{L} is the $1\text{-}\sigma$ error of d_{L} calculated using eq. (2.22), \hat{d}_{L} is the luminosity distance of the GW event. $d_{\text{L}}(z, \boldsymbol{\Omega})$ is the theoretical luminosity distance calculated using eq. (2.1) with z and $\boldsymbol{\Omega}$. $p(z|\boldsymbol{\Omega})$ is the prior distribution of the GW source's redshift z and is given by

$$p(z|\boldsymbol{\Omega}) = \left\{ \frac{1}{N_{\text{in}}} \sum_{j=1}^{N_{\text{in}}} w_j \frac{1}{\sqrt{2\pi}\Delta z(\hat{z}_j)} \exp\left[-\frac{(\hat{z}_j - z)^2}{2(\Delta z(\hat{z}_j))^2}\right] p(\text{G}|z, \boldsymbol{\Omega}) + p(\bar{\text{G}}|z, \boldsymbol{\Omega}) \right\} R_{\text{obs}}(z), \quad (2.31)$$

where $\Delta z(\hat{z}_j)$ is the redshift uncertainties of the j th potential host galaxy, w_j is the angular weight of the j th potential host galaxy calculated using eq. (2.26), and $R_{\text{obs}}(z)$ is the merger rate of SBBHs in the observer frame, obtained by eq. (2.4). $p(\text{G}|z, \boldsymbol{\Omega})$ and $p(\bar{\text{G}}|z, \boldsymbol{\Omega})$ represent the completeness and incompleteness of the galaxy catalog at z , describing the probability of a galaxy at z is in and is not in the galaxy catalog, respectively. We obtain $p(\text{G}|z, \boldsymbol{\Omega})$ from $p(\text{G}|d_{\text{L}})$ through the distance-redshift relation, and $p(\bar{\text{G}}|z, \boldsymbol{\Omega}) = 1 - p(\text{G}|z, \boldsymbol{\Omega})$.

Limited by the observation capability of the survey telescope, the distant and faint galaxy may be ignored by the galaxy catalog, causing the completeness of the galaxy catalog to drop with the distance. To estimate $P(\text{G}|d_{\text{L}}, \boldsymbol{\Omega})$, we first mock galaxies' luminosities by assuming the luminosity distribution of galaxies in the universe can be described by the Schechter function [198], given by

$$p(L) \propto (L/L^*)^\alpha \exp(-L/L^*) dL/L^*, \quad (2.32)$$

where $p(L)$ is the probability of galaxies with luminosity L , $\alpha = -1.07$, and $L^* = 1.2 \times 10^{10} h^{-2} L_{\odot}$ is the characteristic galaxy luminosity, with L_{\odot} being the solar luminosity. Following ref. [103], we set the lower luminosity cutoff for the dimmest galaxies in the universe to $0.001L^*$. The luminosity is then converted to the apparent magnitude, mag , via

$$mag(L, d_{\text{L}}) = Mag_{\odot} - 2.5 \log_{10}^{(L/L_{\odot})} + 5 \log_{10}^{(d_{\text{L}}/\text{pc})} - 5, \quad (2.33)$$

where Mag_{\odot} is the absolute magnitude of the sun. We estimate $P(\text{G}|d_{\text{L}}, \boldsymbol{\Omega})$ by calculating the fraction of galaxies' apparent magnitudes lower than the apparent magnitude threshold in the d_{L} bins with a bin width of 17 Mpc.

Noticeably, in the real observed galaxy catalog, the completeness may vary with the sky localization, so we should calculate $P(\text{G}|d_{\text{L}}, \boldsymbol{\Omega})$ pixel by pixel [103]. In our work, we adopt a simplified assumption that the completeness of the galaxy catalog is uniform in the sky.

The GW selection effect $\beta(\boldsymbol{\Omega})$, as delineated in ref. [99], is considered, expressed as:

$$\beta(\boldsymbol{\Omega}) = \int p_{\text{det}}^{\text{GW}}(d_{\text{L}}(z, \boldsymbol{\Omega})) p(z|\boldsymbol{\Omega}) dz, \quad (2.34)$$

where $p_{\text{det}}^{\text{GW}}(d_{\text{L}}(z, \boldsymbol{\Omega}))$ represents the detection probability of the GW event at $d_{\text{L}}(z, \boldsymbol{\Omega})$, which can be evaluated using Monte-Carlo integration, as explicated in ref. [103],

$$p_{\text{det}}^{\text{GW}}(d_{\text{L}}) = \frac{1}{N_{\text{samp}}} \sum_{n=1}^{N_{\text{samp}}} p_{\text{det}}^{\text{GW}}(d_{\text{L}}|\boldsymbol{\theta}_n), \quad (2.35)$$

with

$$p_{\text{det}}^{\text{GW}}(d_L|\boldsymbol{\theta}_n) \approx \begin{cases} 1, & \text{if } \rho_n > \rho_{\text{th}}, \\ 0, & \text{otherwise,} \end{cases} \quad (2.36)$$

where $N_{\text{samp}} = 50000$ represents the total number of Monte-Carlo realizations, and $\boldsymbol{\theta}_n$ are the GW source parameters other than d_L and z in the n th sampling. We conduct 50000 simulations at each 50 Mpc interval of d_L . When simulating, the source parameters, excluding d_L and z , are drawn from the population models outlined in section 2.2. Ultimately, we derive a smooth curve describing the distribution of $p_{\text{det}}^{\text{GW}}$ along d_L , free from any fluctuations or jitter.

3 Results and discussion

In this section, we show the results of our analysis, including localization errors of GW events and constraints on cosmological parameters, and make relevant discussions.

3.1 Localizations of SBBHs

We show the scatter distributions and cumulative distribution functions (CDFs) of Δd_L , $\Delta\Omega$, and N_{in} in figure 4. In determining d_L , we find that B-DECIGO–ET2CE performs similarly to ET2CE, outperforming B-DECIGO with Δd_L being approximately one order of magnitude smaller. This occurrence is because the measurement of d_L depends on the SNR of the detected signal. The signals of SBBH mainly fall within the detection band of ground-based detectors. Therefore, the measurement error of d_L for ET2CE is smaller than that for B-DECIGO. Moreover, the network composed of B-DECIGO and ET2CE does not show significant enhancement in determining d_L compared to ET2CE alone. For spatial localization, the spatial localization of B-DECIGO–ET2CE is two orders of magnitude better than that of B-DECIGO and ET2CE, and B-DECIGO is nearly an order of magnitude better than ET2CE. The ability of GW detectors to measure d_L and perform spatial angular localization directly influences their search for potential host galaxies. We find that multi-band networked observations can simultaneously enhance the capabilities of measuring d_L and spatial localization, significantly reducing N_{in} . The N_{in} distributions of B-DECIGO and ET2CE are similar, with B-DECIGO performing slightly better, mainly due to its superior spatial localization.

The multi-band synergetic observation of B-DECIGO and ET2CE can significantly improve spatial localization for GW events, which is mainly due to: (i) The multi-band synergetic observation can significantly improve SNR; (ii) The multi-band synergetic observation allows for long-time observation of the GW signal. During this period, the GW detector’s orbital motion enhances spatial positioning accuracy; (iii) The network of space-based and ground-based GW detectors has long baselines, directly boosting the spatial localization.

3.2 Constraints on cosmological parameters

We marginalize d_L and z to infer cosmological parameters. We consider the merger rate distribution discussed in section 2.2 as the population model for GW sources in the redshift prior distribution and assume that we perfectly know the values of population model parameters. In the analysis based on real GW data, a joint inference of cosmological parameters and population model parameters is a better approach [199, 200], due to the poor constraints on population model parameters from current GW observations, and some of these parameters may degenerate with cosmological parameters [112].

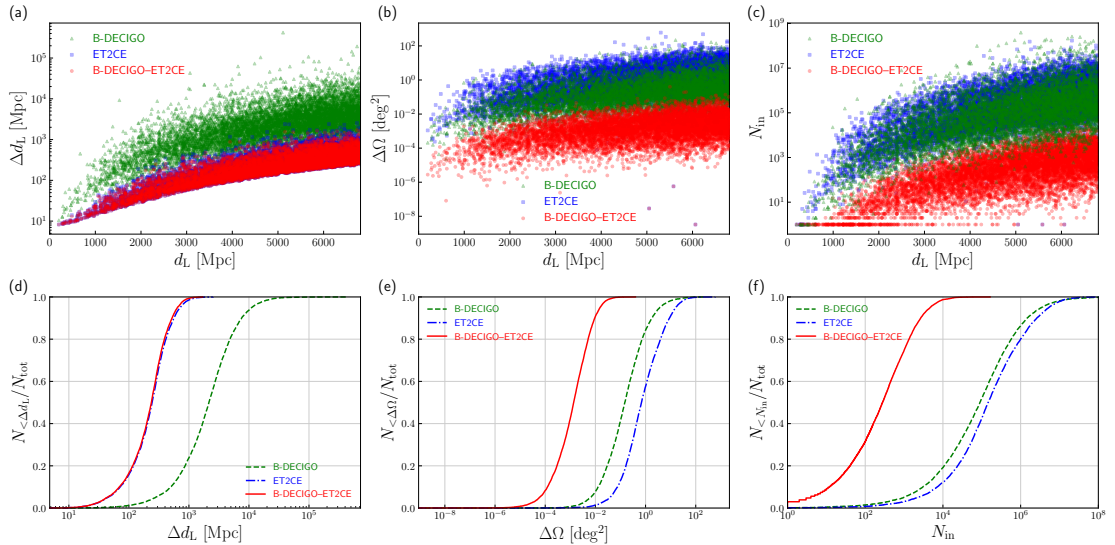


Figure 4. The localization error and the number of potential host galaxies of mock GW events. Panel (a): The results of Δd_L across four GW detector configurations: ET2CE network, B-DECIGO, B-DECIGO–ET2CE network, and LVK network. Panel (b): Similar to panel (a), but showcasing the results for $\Delta\Omega$. Panel (c): Similar to panel (a), but showcasing the number of potential host galaxies N_{in} of each GW event. Panels (d)–(f): CDF of GW events on Δd_L , $\Delta\Omega$, and N_{in} , respectively. In the CDF curve of Δd_L , the y-axis value corresponding to an x-axis value of X represents the proportion of GW events with Δd_L less than X relative to the total number of events, and similarly for the CDF curves of $\Delta\Omega$ and N_{in} .

We only consider GW events at $z \leq 1$, as including larger redshift ranges will drastically increase the number of GW events, leading to excessively long computation times. In fact, the multi-band joint detection of ET2CE and B-DECIGO can detect nearly all GW sources predicted by the population model, with redshifts extending up to $z \sim 10$. Additionally, future galaxy surveys may cover redshift ranges as high as 4 [196]. Therefore, incorporating GW sources with $z > 1$ could further enhance the constraint constraints of cosmological parameters predicted in this study. One potential solution to the issue of excessive computational cost is to use deep learning as an alternative to Bayesian inference [201]. However, this approach falls outside the scope of our current research and may be considered in future studies.

In this study, we investigate the impact of varying levels of catalog completeness by adjusting the apparent magnitude threshold of the mock galaxy catalog to values of 18, 22, 25, and 31. Here, a magnitude threshold of 31 represents a galaxy catalog with 100% completeness at $z \leq 1$. The results presented in table 1, figure 5, and figure 6 are derived using the mock galaxy catalog with a magnitude threshold of 31. Furthermore, we quantify the dependence of the H_0 constraint precision on the magnitude threshold in figure 7, providing insights into how catalog completeness affects cosmological parameter estimation.

Table 1 summarizes the results obtained using a galaxy catalog with 100% completeness at $z \leq 1$. In the first rows, we show the number of GW events with $N_{\text{in}} = 1$. GW events with $N_{\text{in}} = 1$ can be assumed as bright sirens, with redshifts determined by the follow-up

spectroscopic observation. Using the multi-band GW synergetic detection can significantly increase the number of GW events with $N_{\text{in}} = 1$. In the second to fifth rows, we report parameter constraints for H_0 and Ω_m in the Λ CDM model.

Result type	ET	2CE	B-DECIGO	ET2CE	B-DECIGO–ET	B-DECIGO–2CE	B-DECIGO–ET2CE
$N_{\text{in}} = 1$	2	5	15	13	244	257	276
$\sigma(\Omega_m)$	0.083	0.057	0.030	0.026	0.008	0.008	0.007
$\sigma(H_0)$	1.62	1.12	0.62	0.61	0.30	0.29	0.26
$\varepsilon(\Omega_m)$	29.5%	18.8%	9.8%	8.4%	3.4%	3.4%	3.0%
$\varepsilon(H_0)$	2.41%	1.79%	0.89%	0.87%	0.42%	0.42%	0.37%

Table 1. The number of GW events with $N_{\text{in}} = 1$, alongside the absolute errors (1σ) and the relative errors of the cosmological parameters in the Λ CDM model. Here the unit of H_0 is $\text{km s}^{-1} \text{Mpc}^{-1}$.

In figure 5, we present the constraint results of B-DECIGO, ET2CE, and B-DECIGO–ET2CE in the H_0 – Ω plane, using a galaxy catalog with 100% completeness at $z \leq 1$. They depict the optimal situations of the space-based and ground-based detectors and the multi-band GW synergetic detector network, respectively. Using the multi-band GW synergetic detection, B-DECIGO–ET2CE outperforms ET2CE and B-DECIGO, exhibiting enhanced constraint precisions on H_0 by 57.5% and 58.4% and on Ω_m by 64.2% and 69.4%, respectively. Despite B-DECIGO–ET2CE shares a similar Δd_L distribution with ET2CE, as seen in panels (a) and (d) of figure 4, its lower $\Delta\Omega$ leads to the smaller N_{in} , indicating more precise redshift inference than ET2CE, which enhances precision in cosmological parameter constraints through the distance-redshift relation. Compared with B-DECIGO, as shown in figure 4, B-DECIGO–ET2CE has advantages in both Δd_L and $\Delta\Omega$, leading to tighter constraints on cosmological parameters.

In figure 6, we present the H_0 constraint precisions of all GW detector scenarios, based on a galaxy catalog with 100% completeness at $z \leq 1$. 2CE possesses an enhancement of 25.7% over ET. The enhancement of B-DECIGO compared with 2CE is significant, with an H_0 constraint precision enhancement of 50.3%. When using the multi-band GW synergetic detection, the precision constraint precisions of H_0 are below 0.5%, better than the Planck 2018 CMB+BAO result [7]. Even in the worst case of using multi-band GW synergetic detection, B-DECIGO–ET significantly outperforms the best case of not using (ET2CE), with the H_0 constraint precision improved by 51.7%. Notably, with an increasing number of ground-based GW detectors in the multi-band GW synergetic detector network, there are only slight improvements in H_0 constraint precisions. Specifically, with two decimal places retained, the enhancement of B-DECIGO–2CE over B-DECIGO–ET is not visible, and B-DECIGO–ET2CE exhibits a 11.9% improvement over B-DECIGO–2CE. A similar situation also appears in constraining Ω_m , as shown in table 1. The Ω_m constraint precision of B-DECIGO–ET is improved by 59.5% compared with that of ET2CE. Meanwhile, the enhancement of B-DECIGO–2CE over B-DECIGO–ET is also not visible, and B-DECIGO–ET2CE is 11.8% better than B-DECIGO–2CE. Our results indicate that the multi-band GW synergetic observation can significantly enhance the constraint precisions of cosmological parameters and may help resolve the Hubble tension.

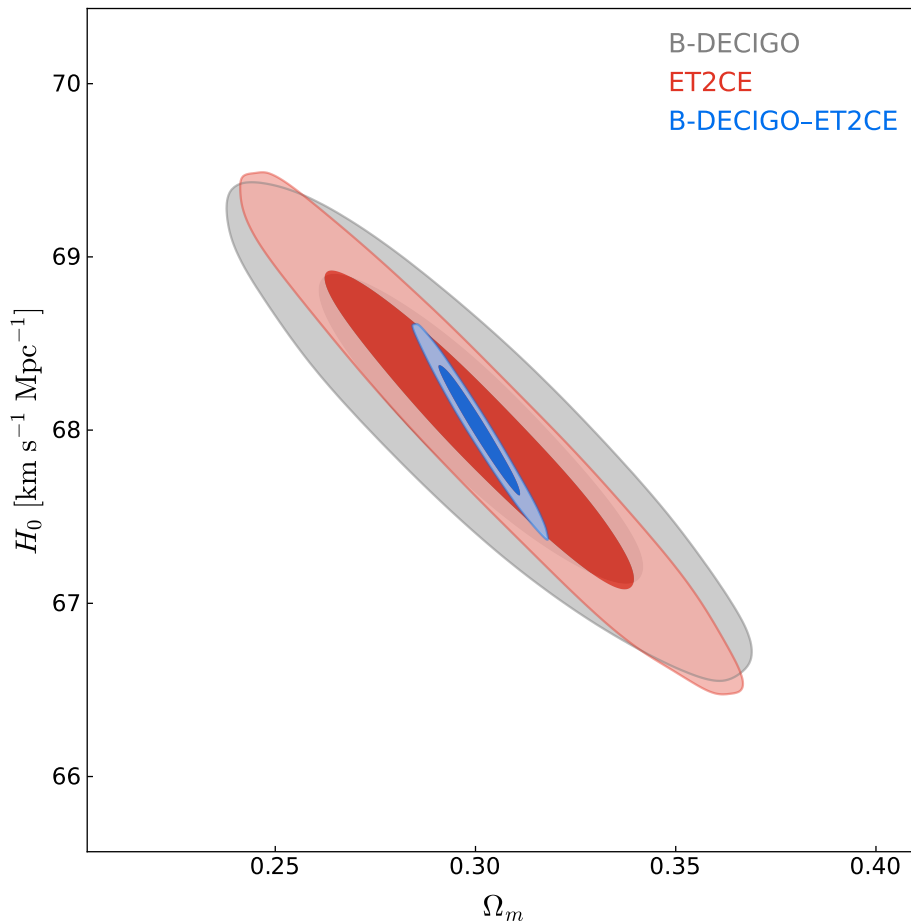


Figure 5. Two-dimensional marginalized contours (68.3% and 95.4% confidence level) in the Ω_m – H_0 plane by using B-DECIGO, ET2CE and B-DECIGO–ET2CE mock data for the Λ CDM model.

In figure 7, we demonstrate the variation in H_0 constraint precisions when adopting different apparent magnitude thresholds. We find that the H_0 constraint precisions decrease as the apparent magnitude threshold decreases and the galaxy catalog’s completeness declines. The thresholds of 18 and 22 roughly represent the upper limits of apparent magnitudes for current survey telescopes, and the threshold of 25 roughly represent the upper limits of apparent magnitudes for future survey telescopes, such as LSST [202, 203] and CSST [197, 204]. From our results, it is evident that the H_0 constraint precisions can be significantly improved with the deployment of future survey projects. When the next-generation survey telescopes become operational, using GW dark sirens could enable an around 1% constraint precision for H_0 and even a sub-precision measurement of H_0 with future GW detector networks, which will provide substantial assistance in resolving the Hubble tension.

4 Conclusion

GW standard sirens have significant potential as a cosmological probe for measuring absolute distances and can constrain the cosmic expansion history through the distance-

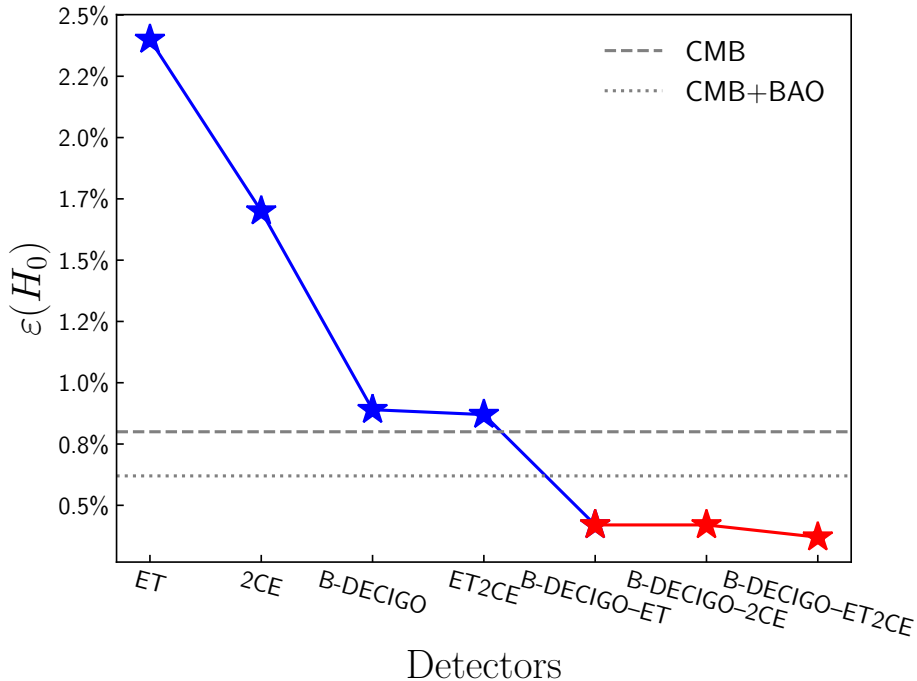


Figure 6. The relative errors of H_0 by using ET, 2CE, B-DECIGO, ET2CE, B-DECIGO–ET, B-DECIGO–2CE, and B-DECIGO–ET2CE mock data. The gray horizontal dashed and point lines represent the constraint precisions of Planck2018 CMB and CMB+BAO data.

redshift relation. The statistical galaxy catalog method provides redshifts for dark sirens without electromagnetic counterparts, relying on GW localization precisions. Multi-band GW synergetic detection can improve SNRs and localization precisions. In this paper, we explore how the multi-band GW synergetic detection of B-DECIGO and 3G ground-based GW detectors enhances dark siren cosmology.

Firstly, we simulate the detection of future GW detectors of SBBH events at $z \leq 1$ in one year using the IMRPhenomD waveform model. Secondly, we use FIM to estimate the localization precisions of B-DECIGO, ET, CEs, and the GW detector networks composed of them. Thirdly, we identify potential host galaxies of dark sirens by cross-matching the GW localization region with a mock galaxy catalog complete up to $z = 1$. We also consider the influence of the completeness of the mock galaxy catalog on our cosmological inference results by setting different apparent magnitude thresholds. Finally, we use Bayesian analysis to infer cosmological parameters in the Λ CDM model.

Our results show that with one year of simulated SMBH GW events, the multi-band GW synergetic observation from B-DECIGO and 3G ground-based GW detectors can constrain H_0 to around 0.4%, showing significant potential in dark siren cosmology. In comparison, without the multi-band synergetic observation strategy, B-DECIGO and 3G ground-based GW detectors can only constrain H_0 to 0.87%–2.41%. Using the multi-band synergetic detection strategy has more than 51% improvement in the constraint precision on H_0 compared with not using it.

We find that multi-band GW synergetic observation enhances dark siren cosmology in the following aspects: (1) Extending the detection frequency range to improve the SNR,

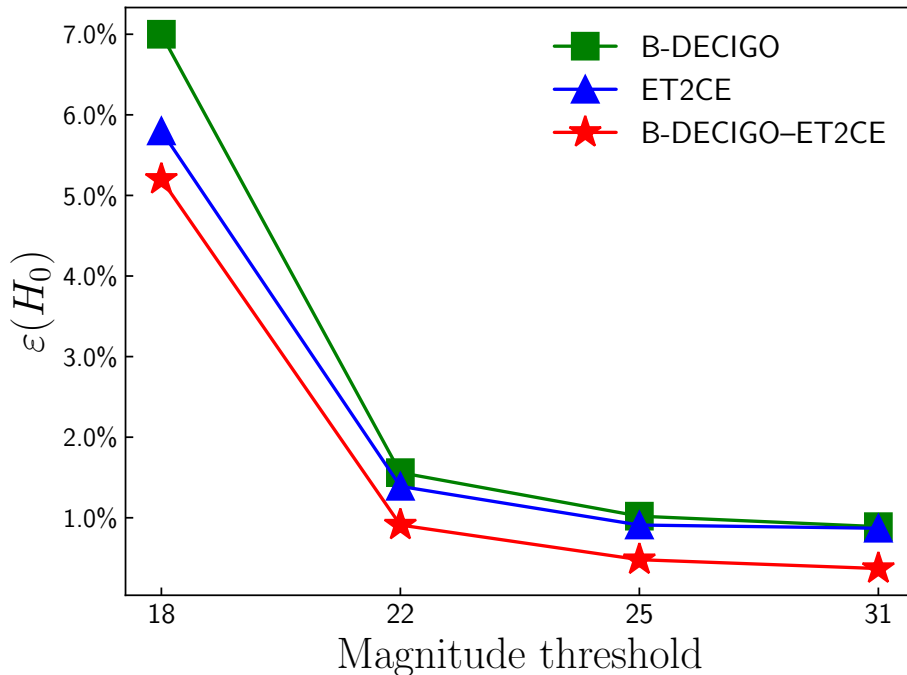


Figure 7. The relative errors of H_0 for different magnitude thresholds by using B-DECIGO, ET2CE and B-DECIGO-ET2CE.

helping us to include more GW events in the dark siren analysis. (2) Enhancing the GW localization precisions, reducing the number of potential host galaxies, and helping to infer the redshifts of dark sirens. (3) Increasing the number of dark sirens with $N_{\text{in}} = 1$, which are de facto bright sirens. We conclude that the multi-band GW synergetic observation has a significant potential enhancement to dark siren cosmology.

Acknowledgements

This work was supported by the National SKA Program of China (Grants Nos. 2022SKA0110200 and 2022SKA0110203), the National Natural Science Foundation of China (Grants Nos. 11975072, 11875102, and 11835009), the National 111 Project (Grant No. B16009), and the China Scholarship Council.

References

- [1] L. Verde, T. Treu and A.G. Riess, *Tensions between the Early and the Late Universe*, *Nature Astron.* **3** (2019) 891 [[1907.10625](#)].
- [2] A.G. Riess, *The Expansion of the Universe is Faster than Expected*, *Nature Rev. Phys.* **2** (2019) 10 [[2001.03624](#)].
- [3] E. Di Valentino, O. Mena, S. Pan, L. Visinelli, W. Yang, A. Melchiorri et al., *In the realm of the Hubble tension—a review of solutions*, *Class. Quant. Grav.* **38** (2021) 153001 [[2103.01183](#)].
- [4] L. Perivolaropoulos and F. Skara, *Challenges for Λ CDM: An update*, *New Astron. Rev.* **95** (2022) 101659 [[2105.05208](#)].

- [5] E. Abdalla et al., *Cosmology intertwined: A review of the particle physics, astrophysics, and cosmology associated with the cosmological tensions and anomalies*, *JHEAp* **34** (2022) 49 [2203.06142].
- [6] M. Kamionkowski and A.G. Riess, *The Hubble Tension and Early Dark Energy*, 2211.04492.
- [7] PLANCK collaboration, *Planck 2018 results. VI. Cosmological parameters*, *Astron. Astrophys.* **641** (2020) A6 [1807.06209].
- [8] A.G. Riess et al., *A Comprehensive Measurement of the Local Value of the Hubble Constant with $1 \text{ km s}^{-1} \text{ Mpc}^{-1}$ Uncertainty from the Hubble Space Telescope and the SH0ES Team*, *Astrophys. J. Lett.* **934** (2022) L7 [2112.04510].
- [9] M. Li, X. Li and X. Zhang, *Comparison of dark energy models: A perspective from the latest observational data*, *Sci. China Phys. Mech. Astron.* **53** (2010) 1631 [0912.3988].
- [10] M. Li, X.-D. Li, Y.-Z. Ma, X. Zhang and Z. Zhang, *Planck Constraints on Holographic Dark Energy*, *JCAP* **09** (2013) 021 [1305.5302].
- [11] J.-F. Zhang, Y.-H. Li and X. Zhang, *Cosmological constraints on neutrinos after BICEP2*, *Eur. Phys. J. C* **74** (2014) 2954 [1404.3598].
- [12] J.-F. Zhang, J.-J. Geng and X. Zhang, *Neutrinos and dark energy after Planck and BICEP2: data consistency tests and cosmological parameter constraints*, *JCAP* **10** (2014) 044 [1408.0481].
- [13] J.-F. Zhang, Y.-H. Li and X. Zhang, *Sterile neutrinos help reconcile the observational results of primordial gravitational waves from Planck and BICEP2*, *Phys. Lett. B* **740** (2015) 359 [1403.7028].
- [14] M.-M. Zhao, D.-Z. He, J.-F. Zhang and X. Zhang, *Search for sterile neutrinos in holographic dark energy cosmology: Reconciling Planck observation with the local measurement of the Hubble constant*, *Phys. Rev. D* **96** (2017) 043520 [1703.08456].
- [15] L. Feng, J.-F. Zhang and X. Zhang, *A search for sterile neutrinos with the latest cosmological observations*, *Eur. Phys. J. C* **77** (2017) 418 [1703.04884].
- [16] W. Yang, S. Pan, E. Di Valentino, R.C. Nunes, S. Vagnozzi and D.F. Mota, *Tale of stable interacting dark energy, observational signatures, and the H_0 tension*, *JCAP* **09** (2018) 019 [1805.08252].
- [17] V. Poulin, T.L. Smith, T. Karwal and M. Kamionkowski, *Early Dark Energy Can Resolve The Hubble Tension*, *Phys. Rev. Lett.* **122** (2019) 221301 [1811.04083].
- [18] R.-Y. Guo, J.-F. Zhang and X. Zhang, *Can the H_0 tension be resolved in extensions to Λ CDM cosmology?*, *JCAP* **02** (2019) 054 [1809.02340].
- [19] E. Di Valentino, A. Melchiorri, O. Mena and S. Vagnozzi, *Interacting dark energy in the early 2020s: A promising solution to the H_0 and cosmic shear tensions*, *Phys. Dark Univ.* **30** (2020) 100666 [1908.04281].
- [20] E. Di Valentino, A. Melchiorri, O. Mena and S. Vagnozzi, *Nonminimal dark sector physics and cosmological tensions*, *Phys. Rev. D* **101** (2020) 063502 [1910.09853].
- [21] M. Liu, Z. Huang, X. Luo, H. Miao, N.K. Singh and L. Huang, *Can Non-standard Recombination Resolve the Hubble Tension?*, *Sci. China Phys. Mech. Astron.* **63** (2020) 290405 [1912.00190].
- [22] X. Zhang and Q.-G. Huang, *Measuring H_0 from low- z datasets*, *Sci. China Phys. Mech. Astron.* **63** (2020) 290402 [1911.09439].
- [23] Q. Ding, T. Nakama and Y. Wang, *A gigaparsec-scale local void and the Hubble tension*, *Sci. China Phys. Mech. Astron.* **63** (2020) 290403 [1912.12600].

- [24] S. Vagnozzi, *New physics in light of the H_0 tension: An alternative view*, *Phys. Rev. D* **102** (2020) 023518 [[1907.07569](#)].
- [25] R.-Y. Guo, J.-F. Zhang and X. Zhang, *Inflation model selection revisited after a 1.91% measurement of the Hubble constant*, *Sci. China Phys. Mech. Astron.* **63** (2020) 290406 [[1910.13944](#)].
- [26] L. Feng, D.-Z. He, H.-L. Li, J.-F. Zhang and X. Zhang, *Constraints on active and sterile neutrinos in an interacting dark energy cosmology*, *Sci. China Phys. Mech. Astron.* **63** (2020) 290404 [[1910.03872](#)].
- [27] H. Li and X. Zhang, *A novel method of measuring cosmological distances using broad-line regions of quasars*, *Sci. Bull.* **65** (2020) 1419 [[2005.10458](#)].
- [28] M.-X. Lin, W. Hu and M. Raveri, *Testing H_0 in Acoustic Dark Energy with Planck and ACT Polarization*, *Phys. Rev. D* **102** (2020) 123523 [[2009.08974](#)].
- [29] S. Mukherjee, B.D. Wandelt, S.M. Nissanke and A. Silvestri, *Accurate precision Cosmology with redshift unknown gravitational wave sources*, *Phys. Rev. D* **103** (2021) 043520 [[2007.02943](#)].
- [30] E. Di Valentino et al., *Snowmass2021 - Letter of interest cosmology intertwined II: The hubble constant tension*, *Astropart. Phys.* **131** (2021) 102605 [[2008.11284](#)].
- [31] L.-Y. Gao, Z.-W. Zhao, S.-S. Xue and X. Zhang, *Relieving the H_0 tension with a new interacting dark energy model*, *JCAP* **07** (2021) 005 [[2101.10714](#)].
- [32] R.-G. Cai, Z.-K. Guo, L. Li, S.-J. Wang and W.-W. Yu, *Chameleon dark energy can resolve the Hubble tension*, *Phys. Rev. D* **103** (2021) 121302 [[2102.02020](#)].
- [33] S. Vagnozzi, *Consistency tests of Λ CDM from the early integrated Sachs-Wolfe effect: Implications for early-time new physics and the Hubble tension*, *Phys. Rev. D* **104** (2021) 063524 [[2105.10425](#)].
- [34] S. Vagnozzi, F. Pacucci and A. Loeb, *Implications for the Hubble tension from the ages of the oldest astrophysical objects*, *JHEAp* **36** (2022) 27 [[2105.10421](#)].
- [35] L.-F. Wang, J.-H. Zhang, D.-Z. He, J.-F. Zhang and X. Zhang, *Constraints on interacting dark energy models from time-delay cosmography with seven lensed quasars*, *Mon. Not. Roy. Astron. Soc.* **514** (2022) 1433 [[2102.09331](#)].
- [36] L.-Y. Gao, S.-S. Xue and X. Zhang, *Dark energy and matter interacting scenario can relieve H_0 and S_8 tensions*, [2212.13146](#).
- [37] Z.-W. Zhao, J.-G. Zhang, Y. Li, J.-M. Zou, J.-F. Zhang and X. Zhang, *First statistical measurement of the Hubble constant using unlocalized fast radio bursts*, [2212.13433](#).
- [38] J.-Z. Qi, Y.-F. Jiang, W.-T. Hou and X. Zhang, *Testing the cosmic distance duality relation using strong gravitational lensing time delays and Type Ia supernovae*, [2407.07336](#).
- [39] G.-H. Du, P.-J. Wu, T.-N. Li and X. Zhang, *Impacts of dark energy on weighing neutrinos after DESI BAO*, [2407.15640](#).
- [40] T.-N. Li, P.-J. Wu, G.-H. Du, S.-J. Jin, H.-L. Li, J.-F. Zhang et al., *Constraints on interacting dark energy models from the DESI BAO and DES supernovae data*, [2407.14934](#).
- [41] N. Dalal, D.E. Holz, S.A. Hughes and B. Jain, *Short grb and binary black hole standard sirens as a probe of dark energy*, *Phys. Rev. D* **74** (2006) 063006 [[astro-ph/0601275](#)].
- [42] C. Cutler and D.E. Holz, *Ultra-high precision cosmology from gravitational waves*, *Phys. Rev. D* **80** (2009) 104009 [[0906.3752](#)].
- [43] S. Nissanke, D.E. Holz, S.A. Hughes, N. Dalal and J.L. Sievers, *Exploring short gamma-ray bursts as gravitational-wave standard sirens*, *Astrophys. J.* **725** (2010) 496 [[0904.1017](#)].

- [44] W. Zhao, C. Van Den Broeck, D. Baskaran and T.G.F. Li, *Determination of Dark Energy by the Einstein Telescope: Comparing with CMB, BAO and SNIa Observations*, *Phys. Rev. D* **83** (2011) 023005 [1009.0206].
- [45] R.-G. Cai and T. Yang, *Estimating cosmological parameters by the simulated data of gravitational waves from the Einstein Telescope*, *Phys. Rev. D* **95** (2017) 044024 [1608.08008].
- [46] R.-G. Cai, Z. Cao, Z.-K. Guo, S.-J. Wang and T. Yang, *The Gravitational-Wave Physics*, *Natl. Sci. Rev.* **4** (2017) 687 [1703.00187].
- [47] R.-G. Cai, T.-B. Liu, X.-W. Liu, S.-J. Wang and T. Yang, *Probing cosmic anisotropy with gravitational waves as standard sirens*, *Phys. Rev. D* **97** (2018) 103005 [1712.00952].
- [48] R.-G. Cai and T. Yang, *Standard sirens and dark sector with Gaussian process*, *EPJ Web Conf.* **168** (2018) 01008 [1709.00837].
- [49] X.-N. Zhang, L.-F. Wang, J.-F. Zhang and X. Zhang, *Improving cosmological parameter estimation with the future gravitational-wave standard siren observation from the Einstein Telescope*, *Phys. Rev. D* **99** (2019) 063510 [1804.08379].
- [50] M. Du, W. Yang, L. Xu, S. Pan and D.F. Mota, *Future constraints on dynamical dark-energy using gravitational-wave standard sirens*, *Phys. Rev. D* **100** (2019) 043535 [1812.01440].
- [51] X. Zhang, *Gravitational wave standard sirens and cosmological parameter measurement*, *Sci. China Phys. Mech. Astron.* **62** (2019) 110431 [1905.11122].
- [52] E. Belgacem, Y. Dirian, S. Foffa, E.J. Howell, M. Maggiore and T. Regimbau, *Cosmology and dark energy from joint gravitational wave-GRB observations*, *JCAP* **08** (2019) 015 [1907.01487].
- [53] M. Safarzadeh, E. Berger, K.K.Y. Ng, H.-Y. Chen, S. Vitale, C. Whittle et al., *Measuring the delay time distribution of binary neutron stars. II. Using the redshift distribution from third-generation gravitational wave detectors network*, *Astrophys. J. Lett.* **878** (2019) L13 [1904.10976].
- [54] J.-F. Zhang, M. Zhang, S.-J. Jin, J.-Z. Qi and X. Zhang, *Cosmological parameter estimation with future gravitational wave standard siren observation from the Einstein Telescope*, *JCAP* **09** (2019) 068 [1907.03238].
- [55] Z. Chang, Q.-G. Huang, S. Wang and Z.-C. Zhao, *Low-redshift constraints on the Hubble constant from the baryon acoustic oscillation “standard rulers” and the gravitational wave “standard sirens”*, *Eur. Phys. J. C* **79** (2019) 177.
- [56] J.-F. Zhang, H.-Y. Dong, J.-Z. Qi and X. Zhang, *Prospect for constraining holographic dark energy with gravitational wave standard sirens from the Einstein Telescope*, *Eur. Phys. J. C* **80** (2020) 217 [1906.07504].
- [57] W. Yang, S. Pan, E. Di Valentino, B. Wang and A. Wang, *Forecasting interacting vacuum-energy models using gravitational waves*, *JCAP* **05** (2020) 050 [1904.11980].
- [58] R.R.A. Bacheaga, A.A. Costa, E. Abdalla and K.S.F. Fornazier, *Forecasting the Interaction in Dark Matter-Dark Energy Models with Standard Sirens From the Einstein Telescope*, *JCAP* **05** (2020) 021 [1906.08909].
- [59] J.-h. He, *Accurate method to determine the systematics due to the peculiar velocities of galaxies in measuring the Hubble constant from gravitational-wave standard sirens*, *Phys. Rev. D* **100** (2019) 023527 [1903.11254].
- [60] Z.-W. Zhao, L.-F. Wang, J.-F. Zhang and X. Zhang, *Prospects for improving cosmological parameter estimation with gravitational-wave standard sirens from Taiji*, *Sci. Bull.* **65** (2020) 1340 [1912.11629].

- [61] L.-F. Wang, Z.-W. Zhao, J.-F. Zhang and X. Zhang, *A preliminary forecast for cosmological parameter estimation with gravitational-wave standard sirens from TianQin*, *JCAP* **11** (2020) 012 [[1907.01838](#)].
- [62] H.-Y. Chen, *Systematic Uncertainty of Standard Sirens from the Viewing Angle of Binary Neutron Star Inspirals*, *Phys. Rev. Lett.* **125** (2020) 201301 [[2006.02779](#)].
- [63] S.-J. Jin, D.-Z. He, Y. Xu, J.-F. Zhang and X. Zhang, *Forecast for cosmological parameter estimation with gravitational-wave standard siren observation from the Cosmic Explorer*, *JCAP* **03** (2020) 051 [[2001.05393](#)].
- [64] S. Borhanian, A. Dhani, A. Gupta, K.G. Arun and B.S. Sathyaprakash, *Dark Sirens to Resolve the Hubble–Lemaître Tension*, *Astrophys. J. Lett.* **905** (2020) L28 [[2007.02883](#)].
- [65] N.B. Hogg, M. Martinelli and S. Nesseris, *Constraints on the distance duality relation with standard sirens*, *JCAP* **12** (2020) 019 [[2007.14335](#)].
- [66] R.C. Nunes, *Searching for modified gravity in the astrophysical gravitational wave background: Application to ground-based interferometers*, *Phys. Rev. D* **102** (2020) 024071 [[2007.07750](#)].
- [67] H.-Y. Chen, P.S. Cowperthwaite, B.D. Metzger and E. Berger, *A Program for Multimessenger Standard Siren Cosmology in the Era of LIGO A+, Rubin Observatory, and Beyond*, *Astrophys. J. Lett.* **908** (2021) L4 [[2011.01211](#)].
- [68] A. Mitra, J. Mifsud, D.F. Mota and D. Parkinson, *Cosmology with the Einstein Telescope: No Slip Gravity Model and Redshift Specifications*, *Mon. Not. Roy. Astron. Soc.* **502** (2021) 5563 [[2010.00189](#)].
- [69] J.-Z. Qi, S.-J. Jin, X.-L. Fan, J.-F. Zhang and X. Zhang, *Using a multi-messenger and multi-wavelength observational strategy to probe the nature of dark energy through direct measurements of cosmic expansion history*, *JCAP* **12** (2021) 042 [[2102.01292](#)].
- [70] X. Fu, L. Zhou, J. Yang, Z.-Y. Lu, Y. Yang and G. Tang, *Exploring the potentiality of future standard candles and standard sirens to detect cosmic opacity*, *Chin. Phys. C* **45** (2021) 065104.
- [71] L. Bian et al., *The Gravitational-wave physics II: Progress*, *Sci. China Phys. Mech. Astron.* **64** (2021) 120401 [[2106.10235](#)].
- [72] C. Ye and M. Fishbach, *Cosmology with standard sirens at cosmic noon*, *Phys. Rev. D* **104** (2021) 043507 [[2103.14038](#)].
- [73] S.-J. Jin, L.-F. Wang, P.-J. Wu, J.-F. Zhang and X. Zhang, *How can gravitational-wave standard sirens and 21-cm intensity mapping jointly provide a precise late-universe cosmological probe?*, *Phys. Rev. D* **104** (2021) 103507 [[2106.01859](#)].
- [74] Z. Guo, *Standard siren cosmology with the lisa-taiji network*, *Science China Physics, Mechanics & Astronomy* **65** (2021) .
- [75] J. Yu, H. Song, S. Ai, H. Gao, F. Wang, Y. Wang et al., *Multimessenger Detection Rates and Distributions of Binary Neutron Star Mergers and Their Cosmological Implications*, *Astrophys. J.* **916** (2021) 54 [[2104.12374](#)].
- [76] M.-D. Cao, J. Zheng, J.-Z. Qi, X. Zhang and Z.-H. Zhu, *A New Way to Explore Cosmological Tensions Using Gravitational Waves and Strong Gravitational Lensing*, *Astrophys. J.* **934** (2022) 108 [[2112.14564](#)].
- [77] J.M.S. de Souza, R. Sturani and J. Alcaniz, *Cosmography with standard sirens from the Einstein Telescope*, *JCAP* **03** (2022) 025 [[2110.13316](#)].
- [78] T. Zhu, W. Zhao and A. Wang, *Polarized primordial gravitational waves in spatial covariant gravities*, [2210.05259](#).

- [79] P.-J. Wu, Y. Shao, S.-J. Jin and X. Zhang, *A path to precision cosmology: synergy between four promising late-universe cosmological probes*, *JCAP* **06** (2023) 052 [[2202.09726](#)].
- [80] S.-J. Jin, R.-Q. Zhu, L.-F. Wang, H.-L. Li, J.-F. Zhang and X. Zhang, *Impacts of gravitational-wave standard siren observations from Einstein Telescope and Cosmic Explorer on weighing neutrinos in interacting dark energy models*, *Commun. Theor. Phys.* **74** (2022) 105404 [[2204.04689](#)].
- [81] L.-F. Wang, Y. Shao, G.-P. Zhang, J.-F. Zhang and X. Zhang, *Ultra-low-frequency gravitational waves from individual supermassive black hole binaries as standard sirens*, [2201.00607](#).
- [82] A. Dhani, S. Borhanian, A. Gupta and B. Sathyaprakash, *Cosmography with bright and Love sirens*, [2212.13183](#).
- [83] E.O. Colgáin, *Probing the Anisotropic Universe with Gravitational Waves*, in *17th Italian-Korean Symposium on Relativistic Astrophysics*, 3, 2022 [[2203.03956](#)].
- [84] W.-T. Hou, J.-Z. Qi, T. Han, J.-F. Zhang, S. Cao and X. Zhang, *Prospects for constraining interacting dark energy models from gravitational wave and gamma ray burst joint observation*, *JCAP* **05** (2023) 017 [[2211.10087](#)].
- [85] M. Califano, I. de Martino, D. Vernieri and S. Capozziello, *Exploiting the Einstein Telescope to solve the Hubble tension*, *Phys. Rev. D* **107** (2023) 123519 [[2208.13999](#)].
- [86] S.-J. Jin, T.-N. Li, J.-F. Zhang and X. Zhang, *Prospects for measuring the Hubble constant and dark energy using gravitational-wave dark sirens with neutron star tidal deformation*, *JCAP* **08** (2023) 070 [[2202.11882](#)].
- [87] S.-J. Jin, S.-S. Xing, Y. Shao, J.-F. Zhang and X. Zhang, *Joint constraints on cosmological parameters using future multi-band gravitational wave standard siren observations**, *Chin. Phys. C* **47** (2023) 065104 [[2301.06722](#)].
- [88] T. Han, S.-J. Jin, J.-F. Zhang and X. Zhang, *A comprehensive forecast for cosmological parameter estimation using joint observations of gravitational-wave standard sirens and short γ -ray bursts*, [2309.14965](#).
- [89] Y.-X. Wang, S.-J. Jin, T.-Y. Sun, J.-F. Zhang and X. Zhang, *Rapid identification of time-frequency domain gravitational wave signals from binary black holes using deep learning*, [2305.19003](#).
- [90] S.-J. Jin, R.-Q. Zhu, J.-Y. Song, T. Han, J.-F. Zhang and X. Zhang, *Standard siren cosmology in the era of the 2.5-generation ground-based gravitational wave detectors: bright and dark sirens of LIGO Voyager and NEMO*, [2309.11900](#).
- [91] S. Vagnozzi, *Seven Hints That Early-Time New Physics Alone Is Not Sufficient to Solve the Hubble Tension*, *Universe* **9** (2023) 393 [[2308.16628](#)].
- [92] T.-N. Li, S.-J. Jin, H.-L. Li, J.-F. Zhang and X. Zhang, *Prospects for Probing the Interaction between Dark Energy and Dark Matter Using Gravitational-wave Dark Sirens with Neutron Star Tidal Deformation*, *Astrophys. J.* **963** (2024) 52 [[2310.15879](#)].
- [93] T. Yang, R.-G. Cai, Z. Cao and H.M. Lee, *Eccentricity enables the earliest warning and localization of gravitational waves with ground-based detectors*, *Phys. Rev. D* **109** (2024) 104041 [[2310.08160](#)].
- [94] J. Zheng, X.-H. Liu and J.-Z. Qi, *Joint observations of late universe probes: cosmological parameter constraints from gravitational wave and Type Ia supernova data*, [2407.05686](#).
- [95] L. Feng, T. Han, J.-F. Zhang and X. Zhang, *Prospects for searching for sterile neutrinos with gravitational wave and γ -ray burst joint observations*, [2409.04453](#).

- [96] B.F. Schutz, *Determining the Hubble Constant from Gravitational Wave Observations*, *Nature* **323** (1986) 310.
- [97] D.E. Holz and S.A. Hughes, *Using gravitational-wave standard sirens*, *Astrophys. J.* **629** (2005) 15 [[astro-ph/0504616](#)].
- [98] W. Del Pozzo, *Inference of the cosmological parameters from gravitational waves: application to second generation interferometers*, *Phys. Rev. D* **86** (2012) 043011 [[1108.1317](#)].
- [99] H.-Y. Chen, M. Fishbach and D.E. Holz, *A two per cent Hubble constant measurement from standard sirens within five years*, *Nature* **562** (2018) 545 [[1712.06531](#)].
- [100] R. Nair, S. Bose and T.D. Saini, *Measuring the Hubble constant: Gravitational wave observations meet galaxy clustering*, *Phys. Rev. D* **98** (2018) 023502 [[1804.06085](#)].
- [101] LIGO SCIENTIFIC, VIRGO collaboration, *A Standard Siren Measurement of the Hubble Constant from GW170817 without the Electromagnetic Counterpart*, *Astrophys. J. Lett.* **871** (2019) L13 [[1807.05667](#)].
- [102] DES, LIGO SCIENTIFIC, VIRGO collaboration, *First Measurement of the Hubble Constant from a Dark Standard Siren using the Dark Energy Survey Galaxies and the LIGO/Virgo Binary-Black-hole Merger GW170814*, *Astrophys. J. Lett.* **876** (2019) L7 [[1901.01540](#)].
- [103] R. Gray et al., *Cosmological inference using gravitational wave standard sirens: A mock data analysis*, *Phys. Rev. D* **101** (2020) 122001 [[1908.06050](#)].
- [104] DES collaboration, *A statistical standard siren measurement of the Hubble constant from the LIGO/Virgo gravitational wave compact object merger GW190814 and Dark Energy Survey galaxies*, *Astrophys. J. Lett.* **900** (2020) L33 [[2006.14961](#)].
- [105] J. Yu, Y. Wang, W. Zhao and Y. Lu, *Hunting for the host galaxy groups of binary black holes and the application in constraining Hubble constant*, *Mon. Not. Roy. Astron. Soc.* **498** (2020) 1786 [[2003.06586](#)].
- [106] LIGO SCIENTIFIC, VIRGO, VIRGO collaboration, *A Gravitational-wave Measurement of the Hubble Constant Following the Second Observing Run of Advanced LIGO and Virgo*, *Astrophys. J.* **909** (2021) 218 [[1908.06060](#)].
- [107] A. Finke, S. Foffa, F. Iacovelli, M. Maggiore and M. Mancarella, *Cosmology with LIGO/Virgo dark sirens: Hubble parameter and modified gravitational wave propagation*, *JCAP* **08** (2021) 026 [[2101.12660](#)].
- [108] H. Leandro, V. Marra and R. Sturani, *Measuring the Hubble constant with black sirens*, *Phys. Rev. D* **105** (2022) 023523 [[2109.07537](#)].
- [109] S. Liu, L.-G. Zhu, Y.-M. Hu, J.-d. Zhang and M.-J. Ji, *Capability for detection of GW190521-like binary black holes with TianQin*, *Phys. Rev. D* **105** (2022) 023019 [[2110.05248](#)].
- [110] T. Yang, R.-G. Cai and H.M. Lee, *Space-borne atom interferometric gravitational wave detections. Part III. Eccentricity on dark sirens*, *JCAP* **10** (2022) 061 [[2208.10998](#)].
- [111] J.-Y. Song, L.-F. Wang, Y. Li, Z.-W. Zhao, J.-F. Zhang, W. Zhao et al., *Synergy between CSST galaxy survey and gravitational-wave observation: Inferring the Hubble constant from dark standard sirens*, [2212.00531](#).
- [112] LIGO SCIENTIFIC, VIRGO, KAGRA collaboration, *Constraints on the Cosmic Expansion History from GWTC-3*, *Astrophys. J.* **949** (2023) 76 [[2111.03604](#)].
- [113] A. Palmese, C.R. Bom, S. Mucesh and W.G. Hartley, *A Standard Siren Measurement of the Hubble Constant Using Gravitational-wave Events from the First Three LIGO/Virgo Observing Runs and the DESI Legacy Survey*, *Astrophys. J.* **943** (2023) 56 [[2111.06445](#)].

- [114] L.-G. Zhu, Y.-M. Hu, H.-T. Wang, J.-d. Zhang, X.-D. Li, M. Hendry et al., *Constraining the cosmological parameters using gravitational wave observations of massive black hole binaries and statistical redshift information*, *Phys. Rev. Res.* **4** (2022) 013247 [2104.11956].
- [115] J.R. Gair et al., *The Hitchhiker’s Guide to the Galaxy Catalog Approach for Dark Siren Gravitational-wave Cosmology*, *Astron. J.* **166** (2023) 22 [2212.08694].
- [116] S. Mukherjee, A. Krolewski, B.D. Wandelt and J. Silk, *Cross-correlating dark sirens and galaxies: measurement of H_0 from GWTC-3 of LIGO-Virgo-KAGRA*, **2203.03643**.
- [117] T. Yang, H.M. Lee, R.-G. Cai, H.G. Choi and S. Jung, *Space-borne atom interferometric gravitational wave detections. Part II. Dark sirens and finding the one*, *JCAP* **01** (2022) 042 [2110.09967].
- [118] T. Yang, R.-G. Cai, Z. Cao and H.M. Lee, *Eccentricity of Long Inspiral Compact Binaries Sheds Light on Dark Sirens*, *Phys. Rev. Lett.* **129** (2022) 191102 [2202.08608].
- [119] N. Muttoni, D. Laghi, N. Tamanini, S. Marsat and D. Izquierdo-Villalba, *Dark siren cosmology with binary black holes in the era of third-generation gravitational wave detectors*, *Phys. Rev. D* **108** (2023) 043543 [2303.10693].
- [120] L.-G. Zhu and X. Chen, *The Dark Side of Using Dark Sirens to Constrain the Hubble–Lemaître Constant*, *Astrophys. J.* **948** (2023) 26 [2302.10621].
- [121] J. Yu, Z. Liu, X. Yang, Y. Wang, P. Zhang, X. Zhang et al., *Measuring the Hubble Constant of Binary Neutron Star and Neutron Star–Black Hole Coalescences: Bright Sirens and Dark Sirens*, *Astrophys. J. Suppl.* **270** (2024) 24 [2311.11588].
- [122] L.-G. Zhu, H.-M. Fan, X. Chen, Y.-M. Hu and J.-d. Zhang, *Improving the Cosmological Constraints by Inferring the Formation Channel of Extreme-mass-ratio Inspirals*, **2403.04950**.
- [123] S.-R. Xiao, Y. Shao, L.-F. Wang, J.-Y. Song, L. Feng, J.-F. Zhang et al., *Nanohertz gravitational waves from a quasar-based supermassive black hole binary population model as dark sirens*, **2408.00609**.
- [124] LIGO SCIENTIFIC, VIRGO collaboration, *GWTC-1: A Gravitational-Wave Transient Catalog of Compact Binary Mergers Observed by LIGO and Virgo during the First and Second Observing Runs*, *Phys. Rev. X* **9** (2019) 031040 [1811.12907].
- [125] LIGO SCIENTIFIC, VIRGO collaboration, *GWTC-2: Compact Binary Coalescences Observed by LIGO and Virgo During the First Half of the Third Observing Run*, *Phys. Rev. X* **11** (2021) 021053 [2010.14527].
- [126] LIGO SCIENTIFIC, VIRGO, KAGRA collaboration, *GWTC-3: Compact Binary Coalescences Observed by LIGO and Virgo During the Second Part of the Third Observing Run*, **2111.03606**.
- [127] LIGO SCIENTIFIC, VIRGO, 1M2H, DARK ENERGY CAMERA GW-E, DES, DLT40, LAS CUMBRES OBSERVATORY, VINROUGE, MASTER collaboration, *A gravitational-wave standard siren measurement of the Hubble constant*, *Nature* **551** (2017) 85 [1710.05835].
- [128] G. Dályá, G. Galgóczi, L. Dobos, Z. Frei, I.S. Heng, R. Macas et al., *GLADE: A galaxy catalogue for multimessenger searches in the advanced gravitational-wave detector era*, *Mon. Not. Roy. Astron. Soc.* **479** (2018) 2374 [1804.05709].
- [129] G. Dályá et al., *GLADE+ : an extended galaxy catalogue for multimessenger searches with advanced gravitational-wave detectors*, *Mon. Not. Roy. Astron. Soc.* **514** (2022) 1403 [2110.06184].
- [130] KAGRA, VIRGO, LIGO SCIENTIFIC collaboration, *GWTC-3: Compact Binary Coalescences Observed by LIGO and Virgo during the Second Part of the Third Observing Run*, *Phys. Rev. X* **13** (2023) 041039 [2111.03606].

- [131] M. Punturo et al., *The Einstein Telescope: A third-generation gravitational wave observatory*, *Class. Quant. Grav.* **27** (2010) 194002.
- [132] LIGO SCIENTIFIC collaboration, *Exploring the Sensitivity of Next Generation Gravitational Wave Detectors*, *Class. Quant. Grav.* **34** (2017) 044001 [1607.08697].
- [133] T. Nakamura, M. Ando, T. Kinugawa, H. Nakano, K. Eda, S. Sato et al., *Pre-DECIGO can get the smoking gun to decide the astrophysical or cosmological origin of GW150914-like binary black holes*, *Progress of Theoretical and Experimental Physics* **2016** (2016) 093E01 [<https://academic.oup.com/ptep/article-pdf/2016/9/093E01/9621962/ptw127.pdf>].
- [134] LISA collaboration, *Laser Interferometer Space Antenna*, **1702.00786**.
- [135] T. Robson, N.J. Cornish and C. Liu, *The construction and use of LISA sensitivity curves*, *Class. Quant. Grav.* **36** (2019) 105011 [1803.01944].
- [136] LISA COSMOLOGY WORKING GROUP collaboration, *Cosmology with the Laser Interferometer Space Antenna*, **2204.05434**.
- [137] W.-R. Hu and Y.-L. Wu, *The Taiji Program in Space for gravitational wave physics and the nature of gravity*, *Natl. Sci. Rev.* **4** (2017) 685.
- [138] Y.-L. Wu, *Hyperunified field theory and Taiji program in space for GWD*, *Int. J. Mod. Phys. A* **33** (2018) 1844014 [1805.10119].
- [139] W.-H. Ruan, Z.-K. Guo, R.-G. Cai and Y.-Z. Zhang, *Taiji program: Gravitational-wave sources*, *Int. J. Mod. Phys. A* **35** (2020) 2050075 [1807.09495].
- [140] TIANQIN collaboration, *TianQin: a space-borne gravitational wave detector*, *Class. Quant. Grav.* **33** (2016) 035010 [1512.02076].
- [141] H.-T. Wang et al., *Science with the TianQin observatory: Preliminary results on massive black hole binaries*, *Phys. Rev. D* **100** (2019) 043003 [1902.04423].
- [142] S. Liu, Y.-M. Hu, J.-d. Zhang and J. Mei, *Science with the TianQin observatory: Preliminary results on stellar-mass binary black holes*, *Phys. Rev. D* **101** (2020) 103027 [2004.14242].
- [143] J. Luo et al., *The first round result from the TianQin-1 satellite*, *Class. Quant. Grav.* **37** (2020) 185013 [2008.09534].
- [144] V.K. Milyukov, *TianQin Space-Based Gravitational Wave Detector: Key Technologies and Current State of Implementation*, *Astron. Rep.* **64** (2020) 1067.
- [145] TIANQIN collaboration, *The TianQin project: current progress on science and technology*, *PTEP* **2021** (2021) 05A107 [2008.10332].
- [146] A. Sesana, *Prospects for Multiband Gravitational-Wave Astronomy after GW150914*, *Phys. Rev. Lett.* **116** (2016) 231102 [1602.06951].
- [147] S. Vitale, *Multiband Gravitational-Wave Astronomy: Parameter Estimation and Tests of General Relativity with Space- and Ground-Based Detectors*, *Phys. Rev. Lett.* **117** (2016) 051102 [1605.01037].
- [148] A. Sesana, *Multi-band gravitational wave astronomy: science with joint space- and ground-based observations of black hole binaries*, *J. Phys. Conf. Ser.* **840** (2017) 012018 [1702.04356].
- [149] S. Isoyama, H. Nakano and T. Nakamura, *Multiband Gravitational-Wave Astronomy: Observing binary inspirals with a decihertz detector, B-DECIGO*, *PTEP* **2018** (2018) 073E01 [1802.06977].
- [150] K. Jani, D. Shoemaker and C. Cutler, *Detectability of Intermediate-Mass Black Holes in Multiband Gravitational Wave Astronomy*, *Nature Astron.* **4** (2019) 260 [1908.04985].

- [151] Z. Carson and K. Yagi, *Parametrized and inspiral-merger-ringdown consistency tests of gravity with multiband gravitational wave observations*, *Phys. Rev. D* **101** (2020) 044047 [[1911.05258](#)].
- [152] C. Liu, L. Shao, J. Zhao and Y. Gao, *Multiband Observation of LIGO/Virgo Binary Black Hole Mergers in the Gravitational-wave Transient Catalog GWTC-1*, *Mon. Not. Roy. Astron. Soc.* **496** (2020) 182 [[2004.12096](#)].
- [153] S. Datta, A. Gupta, S. Kastha, K.G. Arun and B.S. Sathyaprakash, *Tests of general relativity using multiband observations of intermediate mass binary black hole mergers*, *Phys. Rev. D* **103** (2021) 024036 [[2006.12137](#)].
- [154] F. Zhang, X. Chen, L. Shao and K. Inayoshi, *The Eccentric and Accelerating Stellar Binary Black Hole Mergers in Galactic Nuclei: Observing in Ground and Space Gravitational-wave Observatories*, *Astrophys. J.* **923** (2021) 139 [[2109.14842](#)].
- [155] H. Nakano, R. Fujita, S. Isoyama and N. Sago, *Scope out multiband gravitational-wave observations of GW190521-like binary black holes with space gravitational wave antenna B-DECIGO*, *Universe* **7** (2021) 53 [[2101.06402](#)].
- [156] T. Yang, *Gravitational-Wave Detector Networks: Standard Sirens on Cosmology and Modified Gravity Theory*, *JCAP* **05** (2021) 044 [[2103.01923](#)].
- [157] N. Muttoni, A. Mangiagli, A. Sesana, D. Laghi, W. Del Pozzo, D. Izquierdo-Villalba et al., *Multiband gravitational wave cosmology with stellar origin black hole binaries*, *Phys. Rev. D* **105** (2022) 043509 [[2109.13934](#)].
- [158] C. Liu and L. Shao, *Neutron Star–Neutron Star and Neutron Star–Black Hole Mergers: Multiband Observations and Early Warnings*, *Astrophys. J.* **926** (2022) 158 [[2108.08490](#)].
- [159] L.-G. Zhu, L.-H. Xie, Y.-M. Hu, S. Liu, E.-K. Li, N.R. Napolitano et al., *Constraining the Hubble constant to a precision of about 1% using multi-band dark standard siren detections*, *Sci. China Phys. Mech. Astron.* **65** (2022) 259811 [[2110.05224](#)].
- [160] Y. Kang, C. Liu and L. Shao, *Electromagnetic follow-up observations of binary neutron star mergers with early warnings from decihertz gravitational-wave observatories*, *Mon. Not. Roy. Astron. Soc.* **515** (2022) 739 [[2205.02104](#)].
- [161] A. Klein et al., *The last three years: multiband gravitational-wave observations of stellar-mass binary black holes*, [2204.03423](#).
- [162] B.C. Seymour, H. Yu and Y. Chen, *Multiband gravitational wave cosmography with dark sirens*, *Phys. Rev. D* **108** (2023) 044038 [[2208.01668](#)].
- [163] T. Baker, E. Barausse, A. Chen, C. de Rham, M. Pieroni and G. Tasinato, *Testing gravitational wave propagation with multiband detections*, *JCAP* **03** (2023) 044 [[2209.14398](#)].
- [164] Y. Zhao, Y. Lu, C. Yan, Z. Chen and W.-T. Ni, *Multiband gravitational wave observations of stellar binary black holes at the low to middle and high frequencies*, *Mon. Not. Roy. Astron. Soc.* **522** (2023) 2951 [[2306.02636](#)].
- [165] P. Madau and M. Dickinson, *Cosmic Star Formation History*, *Ann. Rev. Astron. Astrophys.* **52** (2014) 415 [[1403.0007](#)].
- [166] KAGRA, VIRGO, LIGO SCIENTIFIC collaboration, *Population of Merging Compact Binaries Inferred Using Gravitational Waves through GWTC-3*, *Phys. Rev. X* **13** (2023) 011048 [[2111.03634](#)].
- [167] S. Vitale, W.M. Farr, K. Ng and C.L. Rodriguez, *Measuring the star formation rate with gravitational waves from binary black holes*, *Astrophys. J. Lett.* **886** (2019) L1 [[1808.00901](#)].
- [168] LIGO SCIENTIFIC, VIRGO collaboration, *Population Properties of Compact Objects from the*

- Second LIGO-Virgo Gravitational-Wave Transient Catalog*, *Astrophys. J. Lett.* **913** (2021) L7 [2010.14533].
- [169] L. Wen and Y. Chen, *Geometrical Expression for the Angular Resolution of a Network of Gravitational-Wave Detectors*, *Phys. Rev. D* **81** (2010) 082001 [1003.2504].
- [170] W. Zhao and L. Wen, *Localization accuracy of compact binary coalescences detected by the third-generation gravitational-wave detectors and implication for cosmology*, *Phys. Rev. D* **97** (2018) 064031 [1710.05325].
- [171] S.A. Usman et al., *The PyCBC search for gravitational waves from compact binary coalescence*, *Class. Quant. Grav.* **33** (2016) 215004 [1508.02357].
- [172] A.H. Nitz, T. Dent, T. Dal Canton, S. Fairhurst and D.A. Brown, *Detecting binary compact-object mergers with gravitational waves: Understanding and Improving the sensitivity of the PyCBC search*, *Astrophys. J.* **849** (2017) 118 [1705.01513].
- [173] G.S. Davies, T. Dent, M. Tápai, I. Harry, C. McIsaac and A.H. Nitz, *Extending the PyCBC search for gravitational waves from compact binary mergers to a global network*, *Phys. Rev. D* **102** (2020) 022004 [2002.08291].
- [174] S. Husa, S. Khan, M. Hannam, M. Pürrer, F. Ohme, X. Jiménez Forteza et al., *Frequency-domain gravitational waves from nonprecessing black-hole binaries. I. New numerical waveforms and anatomy of the signal*, *Phys. Rev. D* **93** (2016) 044006 [1508.07250].
- [175] S. Khan, S. Husa, M. Hannam, F. Ohme, M. Pürrer, X. Jiménez Forteza et al., *Frequency-domain gravitational waves from nonprecessing black-hole binaries. II. A phenomenological model for the advanced detector era*, *Phys. Rev. D* **93** (2016) 044007 [1508.07253].
- [176] B.S. Sathyaprakash and B.F. Schutz, *Physics, Astrophysics and Cosmology with Gravitational Waves*, *Living Rev. Rel.* **12** (2009) 2 [0903.0338].
- [177] K. Yagi and N. Seto, *Detector configuration of DECIGO/BBO and identification of cosmological neutron-star binaries*, *Phys. Rev. D* **83** (2011) 044011 [1101.3940].
- [178] S. Kawamura et al., *Current status of space gravitational wave antenna DECIGO and B-DECIGO*, *PTEP* **2021** (2021) 05A105 [2006.13545].
- [179] A. Krolak, K.D. Kokkotas and G. Schafer, *On estimation of the postNewtonian parameters in the gravitational wave emission of a coalescing binary*, *Phys. Rev. D* **52** (1995) 2089 [gr-qc/9503013].
- [180] A. Buonanno, B. Iyer, E. Ochsner, Y. Pan and B.S. Sathyaprakash, *Comparison of post-Newtonian templates for compact binary inspiral signals in gravitational-wave detectors*, *Phys. Rev. D* **80** (2009) 084043 [0907.0700].
- [181] M. Di Giovanni, C. Giunchi, G. Saccorotti, A. Berbellini, L. Boschi, M. Olivieri et al., *A Seismological Study of the Sos Enattos Area—the Sardinia Candidate Site for the Einstein Telescope*, *Seismological Research Letters* **92** (2020) 352.
- [182] S. Borhanian, *GWBENCH: a novel Fisher information package for gravitational-wave benchmarking*, *Class. Quant. Grav.* **38** (2021) 175014 [2010.15202].
- [183] P. Jaranowski, A. Krolak and B.F. Schutz, *Data analysis of gravitational - wave signals from spinning neutron stars. 1. The Signal and its detection*, *Phys. Rev. D* **58** (1998) 063001 [gr-qc/9804014].
- [184] N. Arnaud, M. Barsuglia, M.-A. Bizouard, P. Canitrot, F. Cavalier, M. Davier et al., *Detection in coincidence of gravitational wave bursts with a network of interferometric detectors. 1. Geometric acceptance and timing*, *Phys. Rev. D* **65** (2002) 042004 [gr-qc/0107081].

- [185] S. Kawamura et al., *The Japanese space gravitational wave antenna DECIGO*, *Class. Quant. Grav.* **23** (2006) S125.
- [186] B.F. Schutz, *Networks of gravitational wave detectors and three figures of merit*, *Class. Quant. Grav.* **28** (2011) 125023 [1102.5421].
- [187] LIGO SCIENTIFIC collaboration, *Advanced LIGO*, *Class. Quant. Grav.* **32** (2015) 074001 [1411.4547].
- [188] LIGO SCIENTIFIC, VIRGO collaboration, *Observing gravitational-wave transient GW150914 with minimal assumptions*, *Phys. Rev. D* **93** (2016) 122004 [1602.03843].
- [189] S. Hild et al., *Sensitivity Studies for Third-Generation Gravitational Wave Observatories*, *Class. Quant. Grav.* **28** (2011) 094013 [1012.0908].
- [190] <https://cosmicexplorer.org/sensitivity.html>.
- [191] L.S. Finn, *Detection, measurement and gravitational radiation*, *Phys. Rev. D* **46** (1992) 5236 [gr-qc/9209010].
- [192] C.M. Hirata, D.E. Holz and C. Cutler, *Reducing the weak lensing noise for the gravitational wave Hubble diagram using the non-Gaussianity of the magnification distribution*, *Phys. Rev. D* **81** (2010) 124046 [1004.3988].
- [193] N. Tamanini, C. Caprini, E. Barausse, A. Sesana, A. Klein and A. Petiteau, *Science with the space-based interferometer eLISA. III: Probing the expansion of the Universe using gravitational wave standard sirens*, *JCAP* **04** (2016) 002 [1601.07112].
- [194] B. Kocsis, Z. Frei, Z. Haiman and K. Menou, *Finding the electromagnetic counterparts of cosmological standard sirens*, *Astrophys. J.* **637** (2006) 27 [astro-ph/0505394].
- [195] E. Barausse, *The evolution of massive black holes and their spins in their galactic hosts*, *Mon. Not. Roy. Astron. Soc.* **423** (2012) 2533 [1201.5888].
- [196] Y. Gong, X. Liu, Y. Cao, X. Chen, Z. Fan, R. Li et al., *Cosmology from the Chinese Space Station Optical Survey (CSS-OS)*, *Astrophys. J.* **883** (2019) 203 [1901.04634].
- [197] Y. Cao et al., *Testing photometric redshift measurements with filter definition of the Chinese Space Station Optical Survey (CSS-OS)*, *Mon. Not. Roy. Astron. Soc.* **480** (2018) 2178 [arXiv:1706.09586 [astro-ph.IM]].
- [198] P. Schechter, *An analytic expression for the luminosity function for galaxies*, *Astrophys. J.* **203** (1976) 297.
- [199] S. Mastrogiovanni, D. Laghi, R. Gray, G.C. Santoro, A. Ghosh, C. Karathanasis et al., *Joint population and cosmological properties inference with gravitational waves standard sirens and galaxy surveys*, *Phys. Rev. D* **108** (2023) 042002 [2305.10488].
- [200] R. Gray et al., *Joint cosmological and gravitational-wave population inference using dark sirens and galaxy catalogues*, *JCAP* **12** (2023) 023 [2308.02281].
- [201] F. Stachurski, C. Messenger and M. Hendry, *Cosmological inference using gravitational waves and normalizing flows*, *Phys. Rev. D* **109** (2024) 123547 [2310.13405].
- [202] LSST collaboration, *LSST: from Science Drivers to Reference Design and Anticipated Data Products*, *Astrophys. J.* **873** (2019) 111 [0805.2366].
- [203] LSST SCIENCE, LSST PROJECT collaboration, *LSST Science Book, Version 2.0*, 0912.0201.
- [204] Y. Cao, Y. Gong, D. Liu, A. Cooray, C. Feng and X. Chen, *Anisotropies of cosmic optical and near-IR background from the China space station telescope (CSST)*, *Mon. Not. Roy. Astron. Soc.* **511** (2022) 1830 [2108.10181].